

NASA TECHNICAL NOTE



NASA TN D-4755

C.J.

LOAN COPY: RETURN
AFWL (WLIL-2)
KIRTLAND AFB, N M

ED 101



NASA TN D-4755

TABLES OF ENERGY AND ANGULAR DISTRIBUTIONS OF THICK TARGET BREMSSTRAHLUNG IN METALS

by Clemans A. Powell, Jr.

Langley Research Center

Langley Station, Hampton, Va.

TECH LIBRARY KAFB, NM



0131703

NASA TN D-4755

TABLES OF ENERGY AND ANGULAR DISTRIBUTIONS
OF THICK TARGET BREMSSTRAHLUNG IN METALS

By Clemans A. Powell, Jr.

Langley Research Center
Langley Station, Hampton, Va.

NATIONAL AERONAUTICS AND SPACE ADMINISTRATION

For sale by the Clearinghouse for Federal Scientific and Technical Information
Springfield, Virginia 22151 - CFSTI price \$3.00

**TABLES OF ENERGY AND ANGULAR DISTRIBUTIONS
OF THICK TARGET BREMSSTRAHLUNG IN METALS**

By Clemans A. Powell, Jr.
Langley Research Center

SUMMARY

Calculations have been made for the angular and energy distributions of bremsstrahlung produced in thick elemental metallic targets by normally incident monoenergetic fluxes of electrons with energies of 0.50, 0.75, 1.00, 2.00, and 3.00 MeV. Results are given for magnesium, aluminum, titanium, manganese, iron, nickel, copper, tungsten, gold, and lead. The target thickness was chosen to be the mean range of the electrons in the particular target material for the electron energy of interest.

The theoretical analysis and resulting computer program by which these data were obtained was reported in NASA Technical Note D-4063. This analysis is based on the approximation of a thick target by a series of thin slabs each of which is considered to be a thin target for bremsstrahlung production, and includes the following secondary processes: (1) the effect of multiple electron scatterings, (2) electron backscatter out of the target, (3) electron-electron bremsstrahlung, and (4) the absorption and buildup of photons in the target.

The results are compared with experimental thick-target bremsstrahlung data for aluminum and iron targets. Although the agreement is generally good, the predicted bremsstrahlung values tend to overestimate the experimental data for low photon energies and underestimate for higher photon energies. The discrepancy between the predicted and experimental values increases with increasing angular displacement from the incident electron direction and with increasing atomic number of the target material.

INTRODUCTION

One of the primary components of the radiation hazards of orbital space flight is due to the energetic electrons trapped in the earth's magnetic field. Not only is the direct exposure to the electron flux a hazard for men and equipment but the very penetrating secondary radiation produced when the electrons' energy is degraded in the spacecraft walls also presents a serious problem. This radiation, called bremsstrahlung, consists of energetic photons created when the electrons are accelerated by the electromagnetic fields of the atomic nuclei and electrons in the spacecraft walls.

The theory for thin-target bremsstrahlung production has been developed such that accurate predictions can be made of the bremsstrahlung produced by a flux of electrons of a given energy provided that each electron makes only one radiative collision in the target, suffers no elastic collisions, and loses essentially no energy to ionization. (See ref. 1.) Most practical spacecraft walls, however, are of such thickness that the electrons would normally suffer a very large number of radiative collisions, lose most of their energy to ionization, and possibly be completely stopped. These conditions greatly increase the difficulty of predicting the bremsstrahlung radiation. In reference 2 a method was presented for estimating the thick-target bremsstrahlung spectrum. This method is based on the assumption that a thick-target bremsstrahlung spectra can be approximated by the summation of spectra from a series of target slabs individually treated as thin targets. Also included in the method are the effects of multiple electron scatterings, electron backscatter, electron-electron bremsstrahlung, and absorption and buildup of photons in the target. The data presented in the tables of the present report are a result of applying this method to additional materials and electron energies and should furnish some needed information for space shielding for electron energies and materials where experimental data are scarce.

The data were computed by the IBM 7094 electronic data processing system at Langley Research Center.

SYMBOLS

A atomic weight of target material

$A_1, A_2 \}$
 $a_1, a_2 \}$ photon buildup coefficients

B photon buildup factor

c	speed of light, centimeter/second (meter/second)
E	total electron energy, m_0c^2 units
ΔE	increment of electron energy, m_0c^2 units
E_m	minimum energy of an electron which can produce a photon of energy k , m_0c^2 units
E_0	incident total electron energy, m_0c^2 units
e	electron charge, statcoulombs (1 coulomb = 2.99790×10^9 statcoulombs)
h	Planck constant, 6.6254×10^{-27} erg-second or 6.6254×10^{-34} joule-second
\bar{I}	average ionization potential, m_0c^2 units
i	index integer of thin-target slabs
k	photon energy, m_0c^2 units
l	index integer for Legendre polynomials
m	limiting number of thin-target slabs over which total bremsstrahlung is summed
m_0	electron rest mass, grams (kilograms)
N_A	Avogadro's number
N_a	target atoms per unit volume, centimeter $^{-3}$ (meter $^{-3}$)
n	integer number of thin-target slabs
P_l	Legendre polynomial
P_ϵ	probability of electron being scattered at angle ϵ

P_γ	probability of emission of a photon in ith thin slab
p	electron momentum, $m_0 c$ units
p_0	initial electron momentum, $m_0 c$ units
R	range of electrons in target material, gram/centimeter ² (kilogram/meter ²)
r_0	classical electron radius, $e^2/m_0 c^2 = 2.82 \times 10^{-13}$ centimeter (10^{-15} meter)
T	electron kinetic energy, million electron volts
T_0	incident electron kinetic energy, million electron volts
t	electron path length, gram/centimeter ² (kilogram/meter ²)
t_x	remaining thickness of target from point of bremsstrahlung production, gram/centimeter ² (kilogram/meter ²)
Δt	increment of path length, gram/centimeter ² (kilogram/meter ²)
v	electron velocity, centimeter/second (meter/second)
v_0	initial electron velocity, centimeter/second (meter/second)
W	ratio of backscattered to incident electrons
X,Y,Z	coordinate axes
Z	atomic number of target material
α	indexing integer for ϵ
β	number of increments in ϵ in each thin slab
γ	indexing integer for ψ
δ	number of increments in ψ in each thin slab

ϵ	angle between electron velocity vector and a normal to target plane
$\Delta\epsilon$	increment in angle ϵ
θ_0	photon emission angle with respect to electron velocity vector
μ_m	photon mass attenuation coefficient, centimeter ² /gram (meter ² /kilogram)
ρ	density of target material, gram/centimeter ³ (kilogram/meter ³)
σ	bremsstrahlung cross section, centimeter ² (meter ²)
σ_e	electron scattering cross section, centimeter ² (meter ²)
φ_d	angle of photon emission with respect to normal to target plane, degrees or radians
ψ	polar angle of electron in thin-target slab, degrees or radians
$\Delta\psi$	increment in angle ψ
Ω	solid angle, steradians

THEORETICAL ANALYSIS

The derivation of equations and associated computer program is presented in reference 2. The following discussion illustrates the basic processes and approximations and show how each process is superposed to give the resulting thick-target bremsstrahlung formula. The following processes are considered:

- (1) the effect of multiple electron scattering
- (2) electron backscatter out of the target
- (3) electron-electron bremsstrahlung
- (4) the absorption and buildup of photons in the target

The basic assumption is that the bremsstrahlung produced in a thick target can be approximated by the sum of bremsstrahlung produced in a series of slabs, each of which can be treated as a thin target.

The radiative collision geometry for an electron impinging on a thin target at some angle ϵ measured from a normal to the plane of the target is shown in figure 1. If a photon is emitted, its direction can be defined by the angles φ_d and θ_0 , where φ_d is the angle between the photon direction and the normal, and θ_0 is the angle between the photon direction and the electron velocity vector. Numerous forms of theoretical bremsstrahlung thin-target cross sections (based on Bethe-Hietler theory) have been tabulated in reference 1. The form used for the calculations presented in this paper (eq. 2BN, ref. 1), which is the differential in photon energy and solid angle, is

$$d\sigma = \frac{Z^2 r_o^2}{8\pi 137} \frac{dk}{k} \frac{p}{p_o} d\Omega \left\{ \frac{8 \sin^2 \theta_0 (2E_o^2 + 1)}{p_o^2 \Delta_o^4} - \frac{2(5E_o^2 + 2EE_o + 3)}{p_o^2 \Delta_o^2} - \frac{2(p_o^2 - k^2)}{Q^2 \Delta_o^2} + \frac{4E}{p_o^2 \Delta_o} \right. \\ + \frac{L}{pp_o} \left[\frac{4E_o \sin^2 \theta_0 (3k - p_o^2 E)}{p_o^2 \Delta_o^4} + \frac{4E_o^2 (E_o^2 + E^2)}{p_o^2 \Delta_o^2} + \frac{2 - 2(7E_o^2 - 3EE_o + E^2)}{p_o^2 \Delta_o^2} \right. \\ \left. \left. + \frac{2k(E_o^2 + EE_o - 1)}{p_o^2 \Delta_o} \right] - \frac{4\epsilon}{p\Delta_o} + \frac{\epsilon Q}{pQ} \left[\frac{4}{\Delta_o^2} - \frac{6k}{\Delta_o} - \frac{2k(p_o^2 - k^2)}{Q^2 \Delta_o} \right] \right\} \quad (1)$$

where

$$L = \log_e \frac{EE_o - 1 + pp_o}{EE_o - 1 - pp_o}$$

$$\Delta_o = E_o - p_o \cos \theta_o$$

$$\epsilon = \log_e \frac{E + p}{E - p}$$

$$\epsilon Q = \log_e \frac{Q + p}{Q - p}$$

$$Q^2 = p_o^2 + k^2 - 2p_o k \cos \theta_o$$

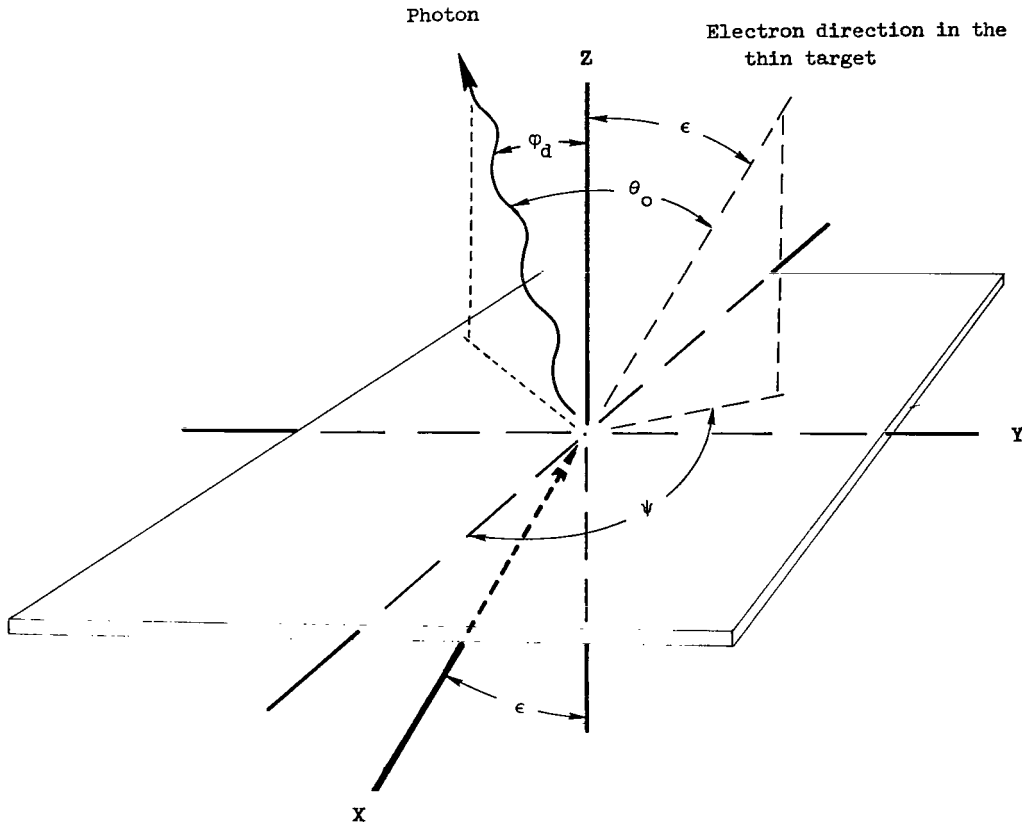


Figure 1.- Electron radiative collision geometry for a thin target.

Equation (1) represents the probability that a photon with energy between k and $k + dk$ will be emitted into a differential solid angle $d\Omega$ oriented in the direction θ_0 from the incident direction of an electron with energy E_0 and momentum p_0 colliding with a thin target with atomic number Z . The total probability P_γ for the emission of a photon of energy between k and $k + dk$ in the direction θ_0 for the sum of the effects of all scattering centers in a thin target of thickness Δt and unit area (for a specified ϵ , ψ , and φ_d) is:

$$P_\gamma(E_i, k, \theta_0) = \left[\frac{d\sigma}{dk d\Omega}(E_i, k, \theta_0) \Delta t N_a \right]_i \quad (2)$$

where N_a is the number of target atoms per unit volume. The angle of photon emission θ_0 with respect to the electron velocity vector is dependent upon the angles ϵ , ψ , and φ_d . This dependence is given by the spherical triangle relationship

$$\cos \theta_0 = \cos \epsilon \cos \varphi_d + \sin \epsilon \sin \varphi_d \cos \psi \quad (3)$$

Multiple Electron Scatterings

Within each thin slab an electron will, in general, suffer many collisions. As a consequence of this multiple electron scattering, the angular distribution of the bremsstrahlung produced is altered. For numerical computation, a convenient expression has been developed by Berger (ref. 3) for the probability P_ϵ of an electron traveling in the ϵ -direction at some point in a thick target after normal initial impingement. Using a Legendre series expansion and assuming a continuous slowing down of the electrons in the absorber, he obtained

$$P_\epsilon(E, \epsilon) = \sum_{l=0}^{\infty} \left(1 + \frac{1}{2}\right) \exp\left[-\int_0^t G_l(t') dt'\right] P_l(\cos \epsilon) \quad (4)$$

where

$$G_l(t') = 2\pi N_a \int_0^\pi \sigma_e(\theta, t') \left[1 - P_l(\cos \theta)\right] \sin \theta d\theta$$

N_a is the number of target atoms per unit volume, t is the path length traversed by the electron, t' is the path-length integration variable, and $\sigma_e(\theta, t')$ is a single-scattering cross section for which the dependence on the electron energy is expressed through the dependence on path length. The average probability of an electron being present in the i th slab at the angle ϵ is given by

$$P_\epsilon = \left[P_\epsilon(E_i, \epsilon) \right]_i \quad (5)$$

Thus for one electron direction of ϵ and ψ , the probability of the production of a photon of energy k which will reach the detector at angle φ_d is the product of the two probabilities (eqs. (2) and (5))

$$P_\gamma P_\epsilon = \left[\frac{d\sigma}{dk d\Omega}(E_i, k, \theta_0) \Delta t N_a P_\epsilon(E_i, \epsilon) \right]_i \quad (6)$$

The total radiative probability in the slab i , if all angles of electron scattering are considered, that is, ϵ varying from 0 to π and ψ varying from 0 to 2π , is

$$\left(\frac{d\sigma}{dk d\Omega} \right)_i = \sum_{\alpha=0}^{\beta} \sum_{\gamma=0}^{\delta} \left[\frac{d\sigma}{dk d\Omega}(E_i, k, \theta_0)_{\alpha, \gamma} \Delta t N_a P_\epsilon(E_i, \frac{\alpha\pi}{\beta}) \sin\left(\frac{\alpha\pi}{\beta}\right) \frac{\pi}{\beta} \frac{2\pi}{\delta} \right]_i$$

where

$$\left. \begin{aligned} \frac{\alpha\pi}{\beta} &= \epsilon \alpha \\ \frac{\pi}{\beta} &= \Delta \epsilon \\ \frac{2\pi}{\delta} &= \Delta \psi \end{aligned} \right\} \quad (7)$$

and α , β , γ , and δ are integers. The dependence of the angle θ_0 and consequently the dependence of the thin-target bremsstrahlung cross sections on the indexing integers α and γ are related through equation (3). The next step is to sum the probabilities over the energy (or the corresponding thickness necessary to bring the electron to rest).

The energy loss of electrons occurs mainly through the different mechanisms of ionizing collisions and radiative collisions. The energy loss per unit path length for all the target materials examined except titanium, manganese, and nickel were obtained from tables prepared by Berger and Seltzer (ref. 4) which consider both ionizing and radiative collisions. For the particular materials of titanium, manganese, and nickel, the energy loss per unit path length was obtained from a relationship developed by Bethe and Ashkin (ref. 5) which considers only energy loss due to ionizing collisions. This relationship is

$$-\frac{dE}{dt} = \frac{2\pi N_a e^4 Z}{m_0 v^2} \left\{ \log_e \left[\frac{m_0 v^2 E}{2\bar{I}^2 \left(1 - \frac{v^2}{c^2} \right)} \right] - \left(2\sqrt{1 - \frac{v^2}{c^2}} - 1 + \frac{v^2}{c^2} \right) \log_e 2 + 1 - \frac{v^2}{c^2} + \frac{1}{8} \left(1 - \sqrt{1 - \frac{v^2}{c^2}} \right)^2 \right\} \quad (8)$$

where m_0 is the electron rest mass, e is the electron charge, v is the electron velocity, c is the speed of light, and \bar{I} is the average ionization potential. Values of the energy loss per unit path length divided by the density of the target materials (called stopping power) are given in table I as functions of the electron energy.

The differential path length in each slab can be expressed as

$$\Delta t = \frac{\Delta E}{dE/dt} \quad (9)$$

Substituting this relation into equations (7) and summing over the number of thin slabs gives

$$\left(\frac{d\sigma}{dk d\Omega} \right)_{\text{Thick target}} = \sum_{i=1}^m \sum_{\alpha=0}^{\beta} \sum_{\gamma=0}^{\delta} \left[\frac{d\sigma}{dk d\Omega}(E_i, k, \theta_0)_{\alpha, \gamma} \frac{N_a}{dE/dt} P_\epsilon(E_i, \frac{\alpha\pi}{\beta}) \sin\left(\frac{\alpha\pi}{\beta}\right) \frac{\pi}{\beta} \frac{2\pi}{\delta} \frac{E_0}{n} \right]_i \quad (10)$$

where $E_0/n = \Delta E$ and n is the number of thin slabs. Since only electrons with total energy greater than $k + m_0 c^2$ can create photons of energy k , the summation must be truncated at $m \leq n$. The governing relationship is

$$E_m \geq k + m_0 c^2 \quad (11a)$$

or

$$E_0 - m \frac{E_0}{n} \geq k + m_0 c^2 \quad (11b)$$

Electron Backscatter

When a beam of electrons strikes a solid target, it has been noted that a significant number of electrons are ejected from the target surface with back-directed velocities. Some of these electrons are a result of secondary emission and have energies in the range of 50 eV or less. A significant number, however, are elastic and inelastic scattered primaries and high-energy secondaries. In reference 6, data are given for the ratios of the high-energy backscattered electrons to the incident electrons. These ratios increase with the atomic number of the target materials and decrease with incident electron energy. Typical ratios range from approximately 0.44 for lead at 1.0 MeV to approximately 0.04 for aluminum at 3.0 MeV. The ratio of the average energy of the backscattered electrons is similarly dependent on the atomic number and electron energy with typical ranges from approximately 0.75 for lead at 1.0 MeV to approximately 0.4 for aluminum at 3.0 MeV. As a result, the total bremsstrahlung production is reduced in proportion to the loss of these high-energy backscattered electrons.

Electron-Electron Bremsstrahlung

In passing through a target material, an electron may also experience collisions with the atomic electrons of the target material. In reference 7 it has been shown that the electron-electron bremsstrahlung may be taken into account with a reasonable degree of accuracy by replacing the Z^2 factor in the thin-target cross-section formula (eq. (1)) by $Z(Z + 1)$.

Absorption and Buildup of Photons

When passing through any material, a photon may interact with the material by the photoelectric effect, Compton scattering, and/or pair production. This interaction gives rise to an exponential attenuation of the photons in the material accompanied by secondary radiations produced by Compton scattered photons, and the radiative decay of the photoelectric electrons and pair-production electrons and positrons. This attenuation and buildup of the photons can be taken into account by the use of a factor which is the ratio of photons at any point to the number of primary photons. This factor can be written as

$$\frac{\text{Number of photons}}{\text{Number of primary photons}} = B(\mu_m t) \exp(-\mu_m t) \quad (12)$$

where

$$B(\mu_m t) = A_1 \exp(-a_1 \mu_m t) + A_2 \exp(-a_2 \mu_m t)$$

t is the material thickness; μ_m is the mass attenuation coefficient at energy k ; and the constants A_1 , a_1 , A_2 , and a_2 are coefficients adjusted to fit experimental or theoretical data. The attenuation coefficients used in the present calculations were obtained with some interpolation from data presented in reference 8 and are given in table II. The buildup coefficients used are given in table III and are interpolations of data given in reference 9.

Thick-Target Cross Section

The processes of backscattering, electron-electron bremsstrahlung and photon absorption and buildup can now be included in the thick-target cross section,

$$\left(\frac{d\sigma}{dk d\Omega} \right)_{\text{Thick target}} = N_a Z(Z+1)(1-W) \sum_{i=1}^m \left[B \exp\left(\frac{-\mu_m t_x}{\cos \varphi_d}\right) \frac{E_0}{n} \sum_{\alpha=0}^{\beta} \sum_{\gamma=0}^{\delta} \frac{1}{Z^2} \frac{d\sigma}{dk d\Omega}(E_i, k, \theta_0)_{\alpha, \gamma} P_\epsilon(E_i, \frac{\alpha\pi}{\beta}) \sin\left(\frac{\alpha\pi}{\beta}\right) \frac{\pi}{\beta} \frac{2\pi}{\delta} \right]_i \quad (13)$$

where $e^{-\mu_m t_x}/\cos \varphi_d$ is the photon attenuation in the target; t_x is the remaining thickness of target material from the point of bremsstrahlung production; B is the photon buildup; $Z(Z+1)$ the approximate correction for electron-electron bremsstrahlung, and W is the ratio of backscattered electrons to incident electrons. If the intensity of bremsstrahlung production is now defined as the photon energy k multiplied by the thick-target cross section, and $N_A \rho / A$ is substituted for N_a , equation (13) becomes

$$\left(k \frac{d\sigma}{dk d\Omega} \right)_{\text{Thick target}} = \frac{N_A}{A} Z(Z+1)(1-W) \sum_{i=1}^m \left[\frac{B \exp\left(\frac{-\mu_m t_X}{\cos \varphi_d}\right)}{\frac{1}{\rho} \frac{dE}{dt}} \frac{E_0}{n} \sum_{\alpha=0}^{\beta} \sum_{\gamma=0}^{\delta} \frac{k}{Z^2} \frac{d\sigma}{dk d\Omega}(E_i, k, \theta_0)_{\alpha, \gamma} P_\epsilon(E_i, \frac{\alpha\pi}{\beta}) \sin\left(\frac{\alpha\pi}{\beta}\right) \frac{\pi}{\beta} \frac{2\pi}{\delta} \right]_i \quad (14)$$

where

$$2\pi \sum_{i=0}^{\beta} P_\epsilon(E_i, \frac{\alpha\pi}{\beta}) \sin\left(\frac{\alpha\pi}{\beta}\right) \frac{\pi}{\beta}$$

has been normalized to one in each thin slab.

RESULTS AND EXPERIMENTAL COMPARISON

The intensity of bremsstrahlung production for thick targets of magnesium, aluminum, titanium, manganese, iron, nickel, copper, tungsten, gold, and lead has been computed for incident electron kinetic energies of 0.50, 0.75, 1.00, 2.00, and 3.00 MeV by using the formula given in equation (14). In all cases the target thickness was chosen equal to the mean range of the incident electrons in the target material. These range values are given in table IV and, except for titanium, manganese, and nickel, were obtained from data presented in reference 4. The ranges for titanium, manganese, and nickel were obtained from the numerical evaluation of the relation

$$R(E_0) = \int_{m_0 c^2}^{E_0} -\frac{1}{\rho} \frac{dE}{dt} \quad (15)$$

where ρ is the density and $-dE/dt$ is the energy loss per unit path length given by equation (8). The bremsstrahlung intensities for the 10 target materials are given in tables V to XIV for detection angles φ_d of 0° , 30° , and 60° from the normal of the target plane.

Little experimental thick-target bremsstrahlung production data exist for the materials and energy ranges examined in this report. Experimental data do exist, however, for aluminum and iron (ref. 10) and some comparisons of the experimental data with the data from tables VI and IX are given in figures 2 to 7.

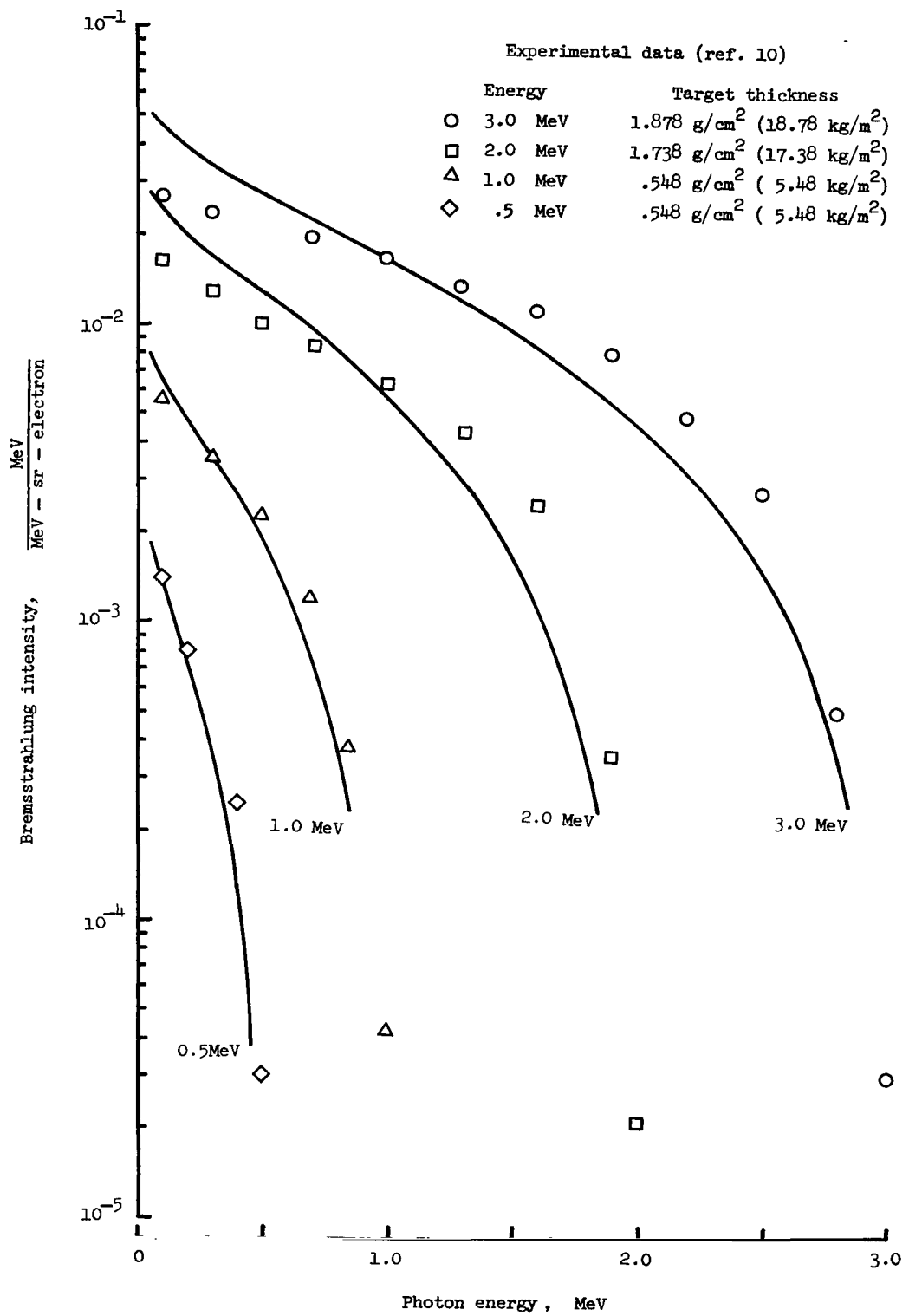


Figure 2.- Bremsstrahlung intensity at 0° for thick aluminum targets.

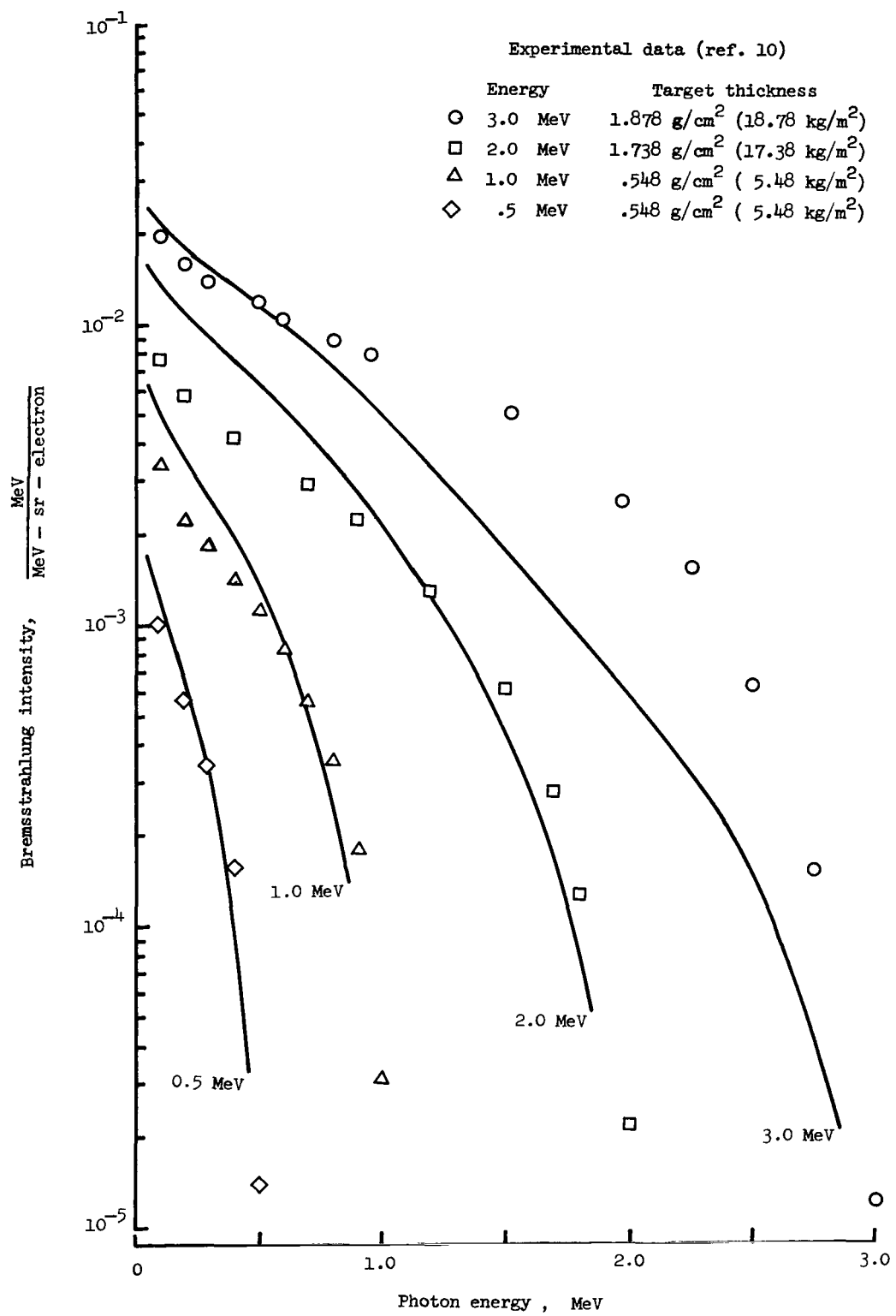


Figure 3.- Bremsstrahlung intensity at 30° for thick aluminum targets.

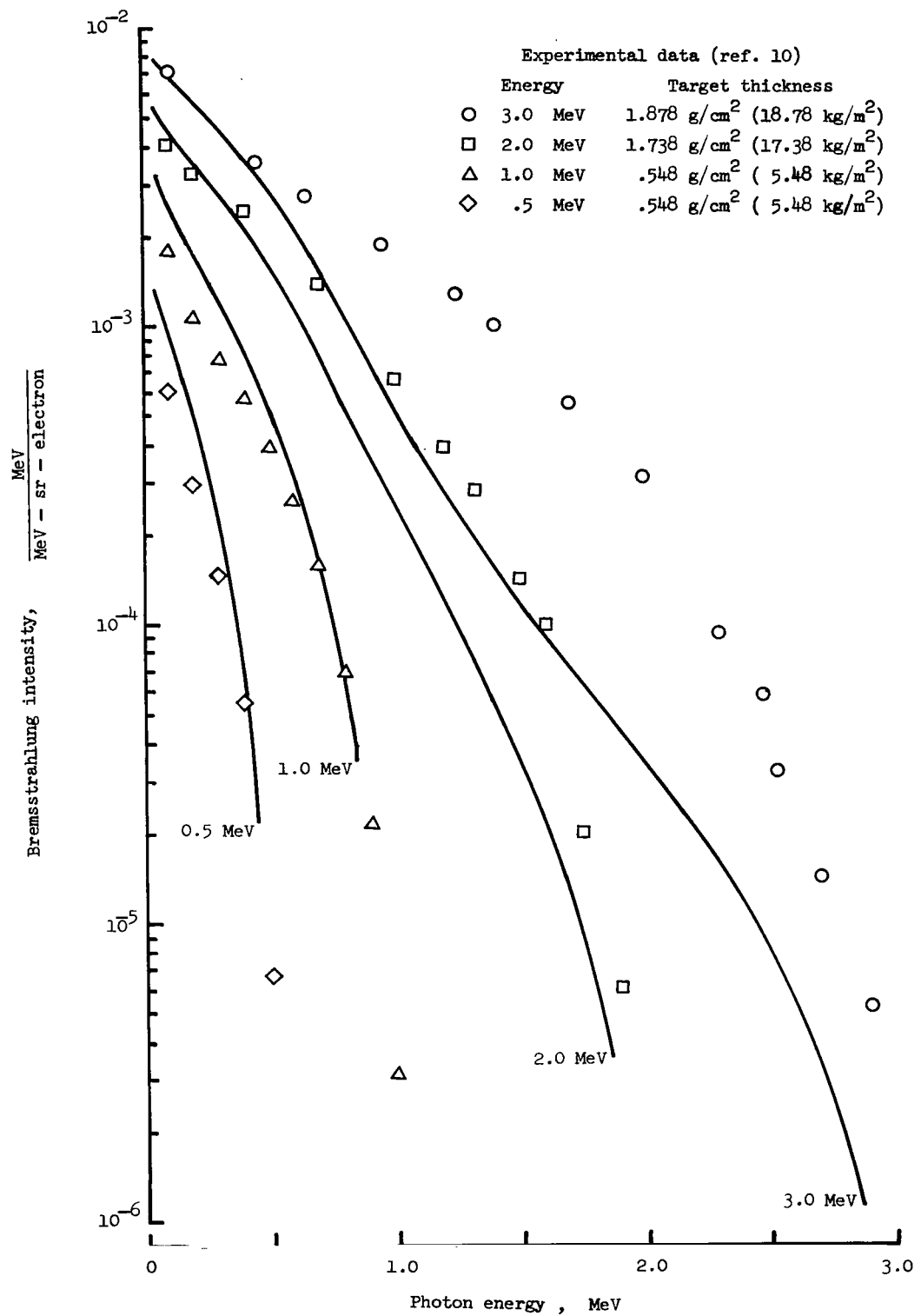


Figure 4.- Bremsstrahlung intensity at 60° for thick aluminum targets.

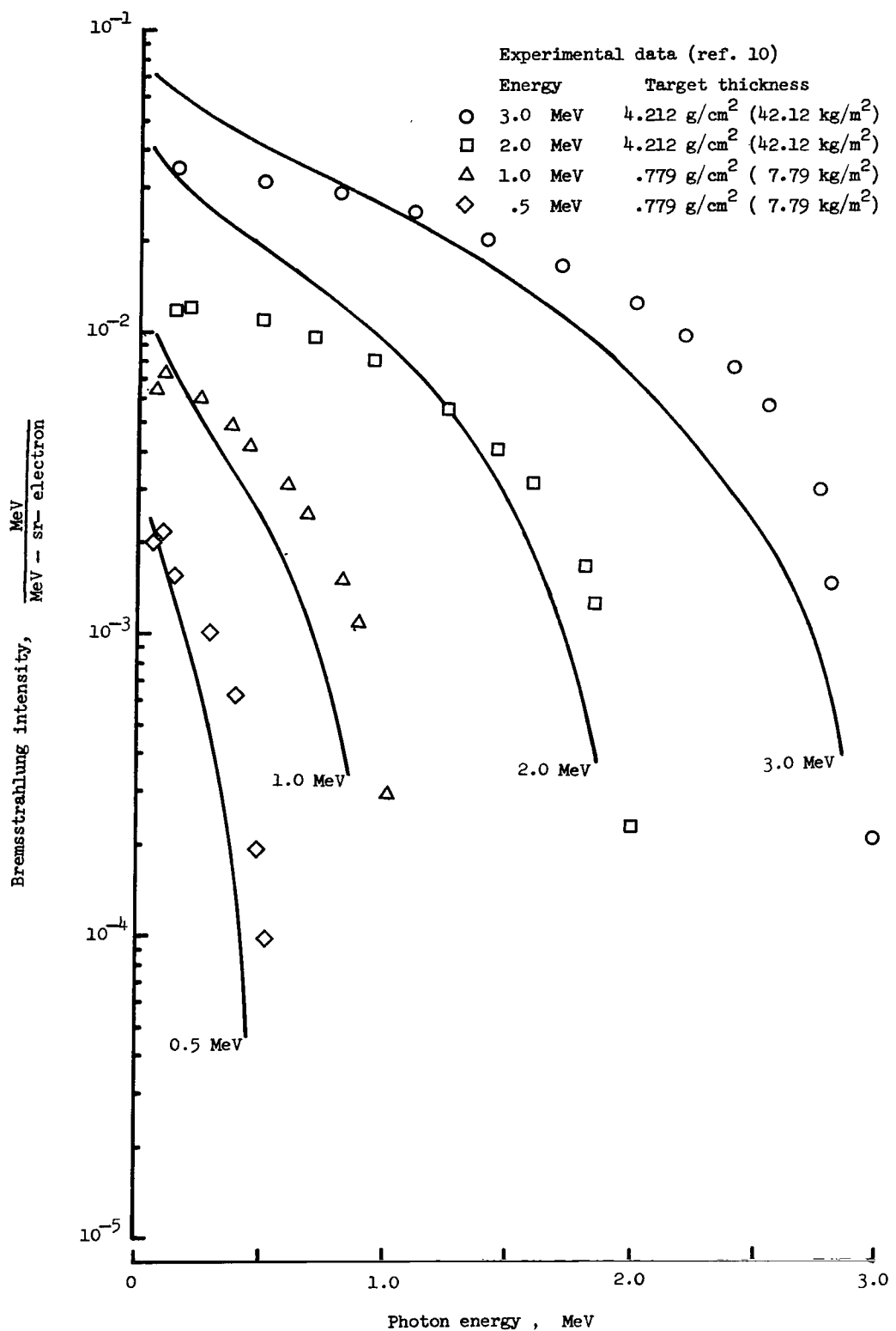


Figure 5.- Bremsstrahlung intensity at 0° for thick iron targets.

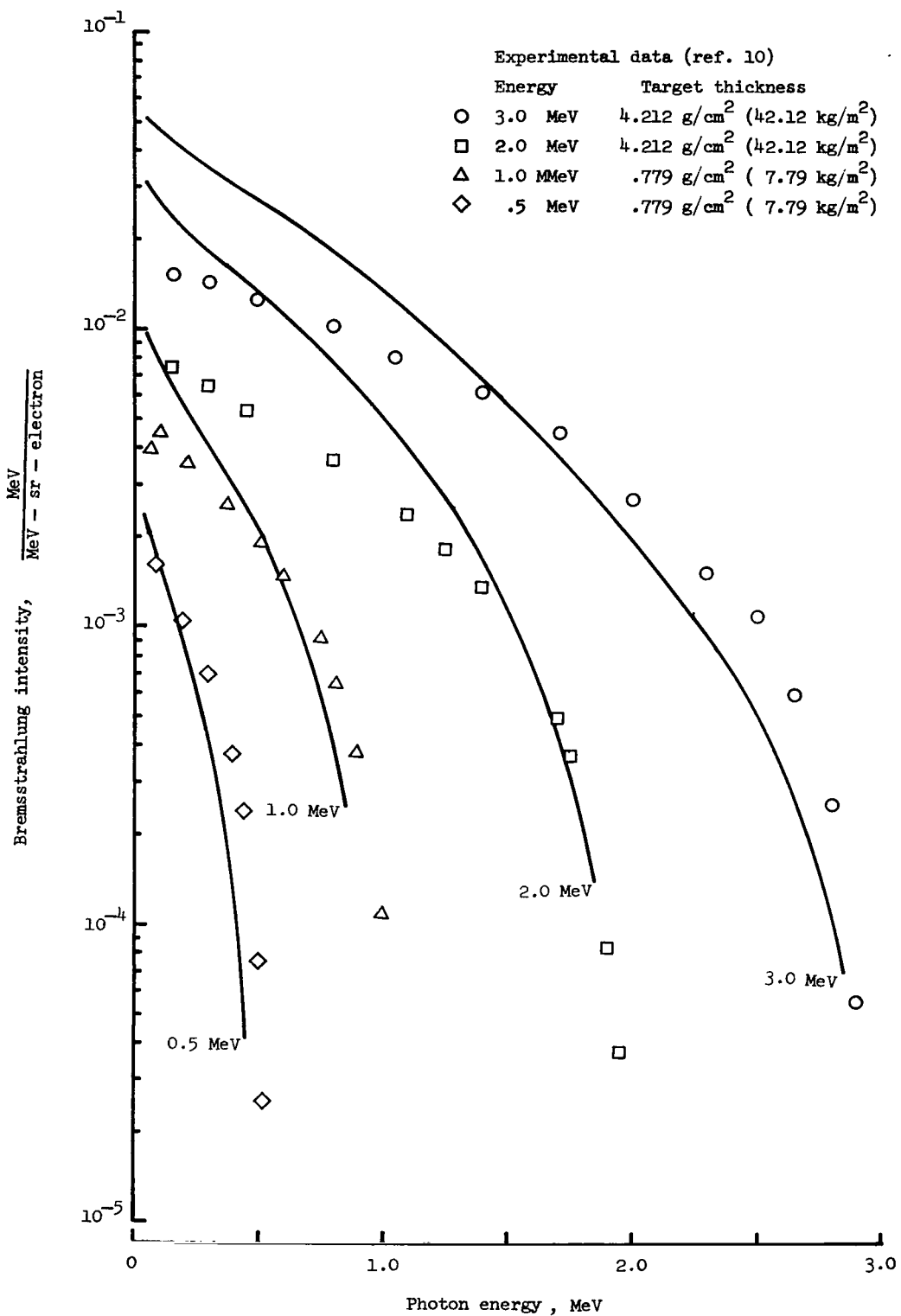


Figure 6.- Bremsstrahlung intensity at 30° for thick iron targets.

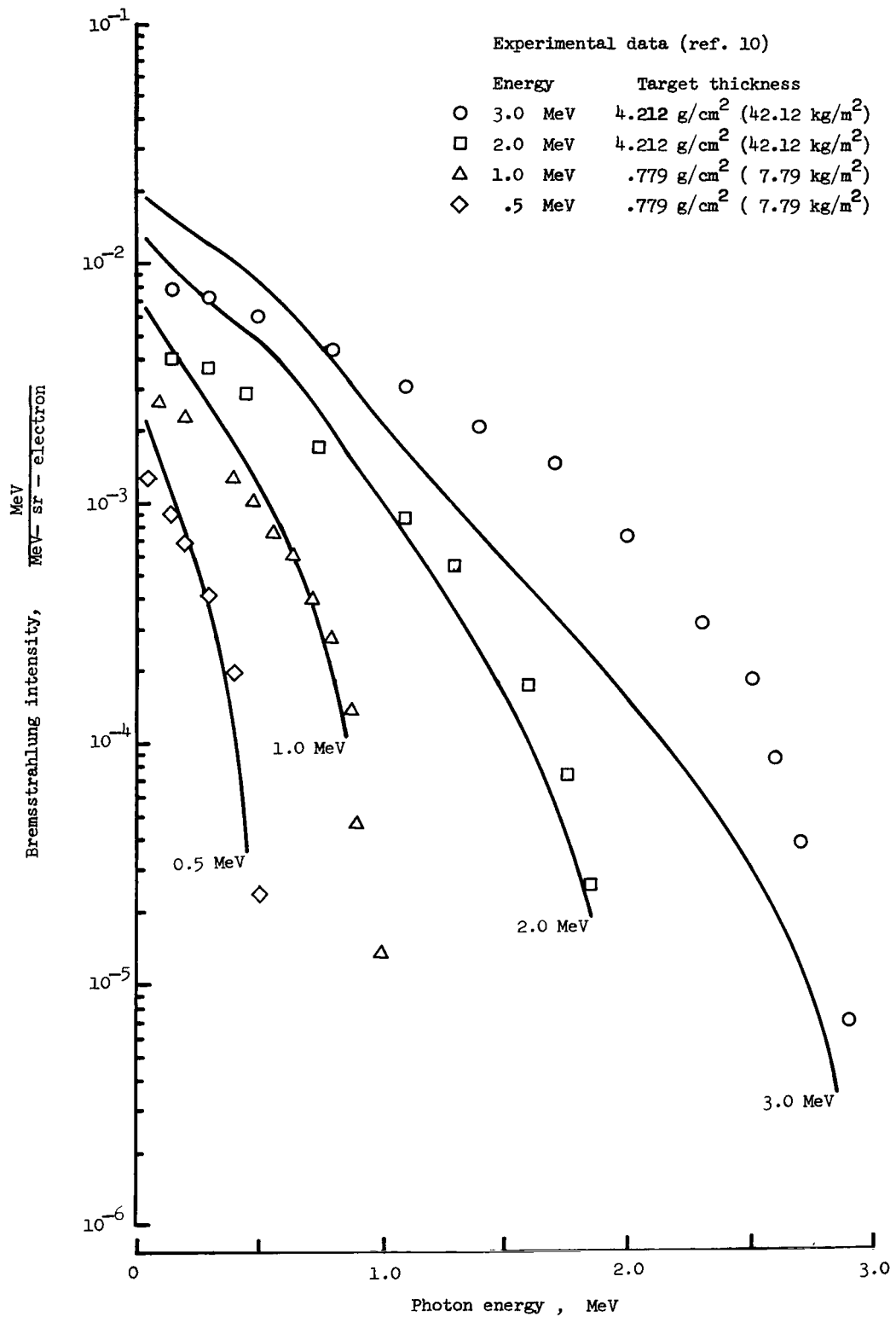


Figure 7.- Bremsstrahlung intensity at 60° for thick iron targets.

The bremsstrahlung intensities presented in these figures are shown as functions of photon energy for incident electron energies of 0.5, 1.0, 2.0, and 3.0 MeV and photon detection angles of 0°, 30°, and 60°. Figures 2 and 5 compare the theoretical calculations with experimental data for aluminum and iron at 0°. The largest differences between experiment and prediction occur for iron in the lower photon energy region. The predicted values generally tend to overestimate the intensity in the lower photon energy range and underestimate for the higher energy ranges; this result might be expected because the thin-target cross-section theoretical equation (eq. (1)) used in the development of this thick-target theory also tends to overestimate the intensity in the lower photon energy range and underestimate in the higher range. The experimental data (from ref. 10) were obtained for iron target thicknesses considerably greater than the mean electron range thickness assumed for the calculations; thus, it would be expected that the attenuation observed in the experiment would be greater than the predicted values, particularly for the lower energy photons. The increase in the discrepancy between prediction and experiment with detection angle is attributed to the use of equation (1), where the same discrepancy occurs in comparison with thin-target data.

There is a somewhat more subtle cause of divergence for the higher atomic number materials. The Bethe-Heitler thin-target cross sections are derived by using the Born approximation technique, which is good provided

$$\frac{2Ze^2}{hv_0} \ll 1 \quad (16)$$

and

$$\frac{2Ze^2}{hv} \ll 1 \quad (17)$$

where v_0 and v are the electron velocities before and after a collision. Because these relations are not as well satisfied for the higher atomic number materials and lower electron velocities, the agreement cannot be expected to be as good.

The buildup factors (table III) were obtained by interpolation between points of the data in reference 9. It is believed that the accuracy of the theoretical predictions could be greatly improved by better buildup input data (from more detailed experimental data rather than by interpolation), especially in the photon energy range below 1 MeV.

CONCLUDING REMARKS

Calculations have been made for the angular and energy distributions of bremsstrahlung produced in thick elemental metallic targets by normally incident monoenergetic

fluxes of electrons with energies of 0.50, 0.75, 1.00, 2.00, and 3.00 MeV. Results are given for magnesium, aluminum, titanium, manganese, iron, nickel, copper, tungsten, gold, and lead. The target thickness was chosen to be the mean range of the electrons in the particular target material for the electron energy of interest.

The theoretical analysis and resulting computer program by which these data were obtained was reported in NASA Technical Note D-4063. This analysis is based on the approximation of a thick target by a series of thin slabs each of which is considered to be a thin target for bremsstrahlung production, and includes the following secondary processes: (1) the effect of multiple electron scatterings, (2) electron backscatter out of the target, (3) electron-electron bremsstrahlung, and (4) the absorption and buildup of photons in the target.

The results are compared with experimental thick-target bremsstrahlung data for aluminum and iron targets. Although the agreement is generally good, the predicted bremsstrahlung values tend to overestimate the experimental data for low photon energies and underestimate for higher photon energies. The discrepancy between the predicted and experimental values increases with increasing angular displacement from the incident electron direction and with increasing atomic number of the target material.

Langley Research Center,
National Aeronautics and Space Administration,
Langley Station, Hampton, Va., April 15, 1968,
124-09-11-03-23.

REFERENCES

1. Koch, H. W.; and Motz, J. W.: Bremsstrahlung Cross-Section Formulas and Related Data. *Rev. Mod. Phys.*, vol. 31, no. 4, Oct. 1959, pp. 920-955.
2. Scott, W. Wayne: Angular Distribution of Thick-Target Bremsstrahlung Which Includes Multiple Electron Scatterings. *NASA TN D-4063*, 1967.
3. Berger, Martin J.: Monte Carlo Calculation of the Penetration and Diffusion of Fast Charged Particles. *Methods in Computational Physics*, Vol. 1 — Statistical Physics, Berni Alder, Sidney Fernbach, and Manuel Rotenberg, eds., Academic Press, 1963, pp. 135-215.
4. Berger, Martin J.; and Seltzer, S. M.: Tables of Energy Losses and Ranges of Electrons and Positrons. *NASA SP-3012*, 1964.
5. Bethe, Hans A.; and Ashkin, Julius: Passage of Radiations Through Matter. *Experimental Nuclear Physics*, Vol. I, E. Segrè, ed., John Wiley & Sons, Inc., c.1953, pp. 166-357.
6. Wright, Kenneth A.; and Trump, John G.: Back-Scattering of Megavolt Electrons From Thick Targets. *J. Appl. Phys.*, vol. 33, no. 2, Feb., 1962, pp. 687-690.
7. Heitler, W.: *The Quantum Theory of Radiation*. Third ed., Clarendon Press (Oxford), 1954.
8. Fano, U.; Zerby, C. D.; and Berger, M. J.: Gamma-Ray Attenuation. Shielding. Vol. III, Pt. B of *Reactor Handbook*, Second ed., Everitt P. Blizzard and Lorraine S. Abbott, eds., Interscience Publ., 1962, pp. 102-127.
9. Taylor, J. J.: Application of Gamma Ray Build-Up Data to Shield Design. *WAPD-RM-217*, Westinghouse Electric Corp., Jan. 25, 1954.
10. Dance, William E.; and Baggerly, Leo L.: Part 1. Bremsstrahlung Production in Aluminum and Iron. *Investigations of Electron Interactions With Matter*, NASA CR-334, 1965, pp. 1-44.

TABLE I.- ELECTRON STOPPING POWER

Target material	Stopping power, MeV cm ² /g (10 ⁻¹ MeV m ² /kg), for -									
	T = 0.1 MeV	T = 0.2 MeV	T = 0.4 MeV	T = 0.6 MeV	T = 0.8 MeV	T = 1.0 MeV	T = 1.5 MeV	T = 2.0 MeV	T = 3.0 MeV	T = 4.0 MeV
Magnesium	3.298	2.264	1.757	1.621	1.572	1.554	1.558	1.583	1.641	1.697
Aluminum	3.200	2.199	1.706	1.571	1.521	1.502	1.505	1.528	1.584	1.639
Titanium	2.847	1.964	1.533	1.414	1.373	1.360	1.377	1.394	1.449	1.496
Manganese	2.783	1.922	1.502	1.387	1.347	1.334	1.350	1.370	1.424	1.471
Iron	2.857	1.984	1.557	1.443	1.405	1.394	1.411	1.447	1.527	1.605
Nickel	2.860	1.980	1.549	1.432	1.391	1.380	1.395	1.418	1.475	1.524
Copper	2.738	1.908	1.508	1.398	1.364	1.356	1.378	1.417	1.502	1.584
Tungsten	2.091	1.501	1.229	1.174	1.169	1.180	1.242	1.316	1.464	1.608
Gold	2.063	1.486	1.221	1.168	1.165	1.177	1.242	1.319	1.475	1.625
Lead	2.024	1.461	1.203	1.152	1.153	1.168	1.238	1.316	1.476	1.630

TABLE II.- MASS ATTENUATION COEFFICIENTS

Target material	Mass attenuation coefficients, cm ² /g (10 ⁻¹ m ² /kg), for -									
	T = 0.1 MeV	T = 0.2 MeV	T = 0.4 MeV	T = 0.6 MeV	T = 0.8 MeV	T = 1.0 MeV	T = 1.5 MeV	T = 2.0 MeV	T = 3.0 MeV	T = 4.0 MeV
Magnesium	0.160	0.122	0.0944	0.0795	0.0699	0.0627	0.0512	0.0442	0.0360	0.0315
Aluminum	.161	.120	.0922	.0777	.0683	.0614	.0500	.0432	.0353	.0310
Titanium	.275	.134	.0952	.0803	.0696	.0625	.0505	.0431	.0372	.0335
Manganese	.328	.137	.0929	.0775	.0675	.0602	.0490	.0423	.0363	.0331
Iron	.344	.138	.0919	.0762	.0664	.0595	.0485	.0424	.0360	.0330
Nickel	.386	.144	.0915	.0764	.0660	.0587	.0478	.0419	.0350	.0330
Copper	.427	.147	.0916	.0751	.0654	.0585	.0476	.0418	.0357	.0330
Tungsten	4.21	.708	.174	.101	.0763	.0640	.0492	.0437	.0405	.0402
Gold	4.88	.878	.195	.109	.0809	.0665	.0503	.0447	.0416	.0413
Lead	5.29	.896	.208	.114	.0836	.0684	.0512	.0457	.0421	.0420

TABLE III.- PHOTON BUILDUP COEFFICIENTS OF TARGET MATERIALS

Photon energy, MeV	Buildup coefficients				Photon energy, MeV	Buildup coefficients			
	A ₁	-a ₁	-A ₂	a ₂		A ₁	-a ₁	-A ₂	a ₂
Magnesium									
1.0	11.5	0.094	10.5	0.017	1.0	8.7	0.080	7.7	0.028
1.5	7.9	.076	6.9	.050	1.5	7.1	.076	6.1	.033
2.0	6.3	.068	5.3	.072	2.0	5.9	.074	4.9	.039
3.0	4.7	.059	3.7	.094	3.0	4.2	.074	3.2	.052
4.0	3.9	.054	2.9	.105	4.0	3.4	.075	2.4	.063
Aluminum									
1.0	11.3	0.093	10.3	0.017	1.0	8.6	0.079	7.6	0.028
1.5	7.9	.077	6.9	.045	1.5	7.0	.076	6.0	.033
2.0	6.3	.069	5.3	.065	2.0	5.9	.074	4.9	.039
3.0	4.7	.060	3.7	.088	3.0	4.2	.072	3.2	.051
4.0	3.9	.057	2.9	.100	4.0	3.4	.076	2.4	.063
Titanium									
1.0	9.6	0.085	8.6	0.023	1.0	3.3	0.044	2.3	0.11
1.5	7.6	.076	6.6	.033	1.5	3.4	.053	2.4	.12
2.0	6.1	.072	5.1	.043	2.0	3.3	.062	2.3	.12
3.0	4.4	.070	3.4	.059	3.0	2.7	.081	1.7	.11
4.0	3.6	.069	2.6	.070	4.0	2.0	.10	.96	.11
Manganese									
1.0	9.1	0.083	8.1	0.025	1.0	2.9	0.040	1.9	0.13
1.5	7.3	.076	6.3	.033	1.5	3.0	.049	2.0	.13
2.0	6.0	.073	5.0	.041	2.0	2.9	.059	1.9	.13
3.0	4.3	.072	3.3	.054	3.0	2.4	.080	1.4	.13
4.0	3.6	.072	2.6	.066	4.0	1.8	.10	.80	.12
Iron									
1.0	9.0	0.082	8.0	0.026	1.0	2.7	0.038	1.7	0.14
1.5	7.3	.077	6.3	.033	1.5	2.7	.044	1.7	.14
2.0	6.0	.074	5.0	.040	2.0	2.7	.057	1.7	.14
3.0	4.5	.073	3.5	.053	3.0	2.2	.080	1.2	.13
4.0	3.5	.073	2.5	.065	4.0	1.7	.11	.70	.13
Nickel									
Copper									
Tungsten									
Gold									
Lead									

TABLE IV.- MEAN ELECTRON RANGE

Target material	Mean electron range, g/cm ² (0.1 kg/m ²), for -				
	T _O = 3.00 MeV	T _O = 2.00 MeV	T _O = 1.00 MeV	T _O = 0.75 MeV	T _O = 0.50 MeV
Magnesium	1.793	1.173	0.532	0.373	0.218
Aluminum	1.855	1.212	.549	.384	.224
Titanium	2.044	1.340	.611	.428	.250
Manganese	2.084	1.367	.624	.437	.256
Iron	1.980	1.307	.598	.421	.248
Nickel	2.010	1.320	.603	.423	.248
Copper	2.030	1.344	.620	.436	.257
Tungsten	2.273	1.553	.748	.535	.322
Gold	2.274	1.558	.753	.539	.325
Lead	2.288	1.571	.763	.547	.330

TABLE V.- THICK-TARGET BREMSSTRAHLUNG INTENSITY FOR MAGNESIUM

Photon energy, MeV	Bremsstrahlung intensity, $\frac{\text{MeV}}{\text{MeV}\cdot\text{sr}\cdot\text{electron}}$		
	$\varphi_d = 0^\circ$	$\varphi_d = 30^\circ$	$\varphi_d = 60^\circ$
$T_0 = 3.00 \text{ MeV}$			
0.05	4.56×10^{-2}	2.15×10^{-2}	7.08×10^{-3}
.15	3.71×10^{-2}	1.69×10^{-2}	5.34×10^{-3}
.25	3.22×10^{-2}	1.42×10^{-2}	4.28×10^{-3}
.35	2.88×10^{-2}	1.25×10^{-2}	3.53×10^{-3}
.45	2.60×10^{-2}	1.09×10^{-2}	2.73×10^{-3}
.65	2.14×10^{-2}	7.97×10^{-3}	1.43×10^{-3}
.85	1.75×10^{-2}	5.58×10^{-3}	6.93×10^{-4}
1.05	1.42×10^{-2}	3.76×10^{-3}	3.52×10^{-4}
1.25	1.14×10^{-2}	2.48×10^{-3}	1.90×10^{-4}
1.45	8.92×10^{-3}	1.62×10^{-3}	1.09×10^{-4}
1.65	6.89×10^{-3}	1.05×10^{-3}	6.55×10^{-5}
1.85	5.19×10^{-3}	6.79×10^{-4}	4.03×10^{-5}
2.05	3.76×10^{-3}	4.28×10^{-4}	2.48×10^{-5}
2.25	2.55×10^{-3}	2.58×10^{-4}	1.44×10^{-5}
2.45	1.56×10^{-3}	1.44×10^{-4}	7.93×10^{-6}
2.65	7.72×10^{-4}	6.74×10^{-5}	3.66×10^{-6}
2.85	2.17×10^{-4}	1.82×10^{-5}	9.53×10^{-7}
$T_0 = 2.00 \text{ MeV}$			
0.05	2.61×10^{-2}	1.44×10^{-2}	4.82×10^{-3}
.15	2.01×10^{-2}	1.09×10^{-2}	3.48×10^{-3}
.25	1.68×10^{-2}	8.88×10^{-3}	2.70×10^{-3}
.35	1.45×10^{-2}	7.45×10^{-3}	2.09×10^{-3}
.45	1.26×10^{-2}	6.24×10^{-3}	1.56×10^{-3}
.65	9.41×10^{-3}	4.19×10^{-3}	7.70×10^{-4}
.85	6.86×10^{-3}	2.66×10^{-3}	3.58×10^{-4}
1.05	4.78×10^{-3}	1.59×10^{-3}	1.69×10^{-4}
1.25	3.10×10^{-3}	8.89×10^{-4}	7.90×10^{-5}
1.45	1.79×10^{-3}	4.49×10^{-4}	3.54×10^{-5}
1.65	8.27×10^{-4}	1.87×10^{-4}	1.38×10^{-5}
1.85	2.08×10^{-4}	4.43×10^{-5}	3.16×10^{-6}
Photon energy, MeV	Bremsstrahlung intensity, $\frac{\text{MeV}}{\text{MeV}\cdot\text{sr}\cdot\text{electron}}$		
	$\varphi_d = 0^\circ$	$\varphi_d = 30^\circ$	$\varphi_d = 60^\circ$
$T_0 = 1.00 \text{ MeV}$			
0.05	7.83×10^{-3}	6.02×10^{-3}	3.00×10^{-3}
.15	5.27×10^{-3}	3.99×10^{-3}	1.92×10^{-3}
.25	3.90×10^{-3}	2.90×10^{-3}	1.32×10^{-3}
.35	2.93×10^{-3}	2.12×10^{-3}	8.93×10^{-4}
.45	2.13×10^{-3}	1.49×10^{-3}	5.67×10^{-4}
.65	9.36×10^{-4}	6.03×10^{-4}	1.82×10^{-4}
.85	2.18×10^{-4}	1.28×10^{-4}	3.25×10^{-5}
$T_0 = 0.75 \text{ MeV}$			
0.05	3.28×10^{-3}	2.79×10^{-3}	1.72×10^{-3}
.15	2.03×10^{-3}	1.70×10^{-3}	1.02×10^{-3}
.25	1.36×10^{-3}	1.12×10^{-3}	6.38×10^{-4}
.35	9.02×10^{-4}	7.25×10^{-4}	3.83×10^{-4}
.45	5.40×10^{-4}	4.20×10^{-4}	2.02×10^{-4}
.65	8.36×10^{-5}	6.03×10^{-5}	2.45×10^{-5}
$T_0 = 0.50 \text{ MeV}$			
0.05	9.36×10^{-4}	8.70×10^{-4}	6.82×10^{-4}
.15	4.87×10^{-4}	4.47×10^{-4}	3.42×10^{-4}
.25	2.56×10^{-4}	2.31×10^{-4}	1.69×10^{-4}
.35	1.09×10^{-4}	9.56×10^{-5}	6.55×10^{-5}
.45	1.86×10^{-5}	1.57×10^{-5}	1.01×10^{-5}

TABLE VI.- THICK-TARGET BREMSSTRAHLUNG INTENSITY FOR ALUMINUM

Photon energy, MeV	Bremsstrahlung intensity, $\frac{\text{MeV}}{\text{MeV-sr-electron}}$		
	$\varphi_d = 0^\circ$	$\varphi_d = 30^\circ$	$\varphi_d = 60^\circ$
$T_0 = 3.00 \text{ MeV}$			
0.05	5.06×10^{-2}	2.46×10^{-2}	7.95×10^{-3}
.15	4.08×10^{-2}	1.94×10^{-2}	6.27×10^{-3}
.25	3.55×10^{-2}	1.65×10^{-2}	5.14×10^{-3}
.35	3.18×10^{-2}	1.44×10^{-2}	4.17×10^{-3}
.45	2.87×10^{-2}	1.26×10^{-2}	3.31×10^{-3}
.65	2.36×10^{-2}	9.33×10^{-3}	1.81×10^{-3}
.85	1.94×10^{-2}	6.60×10^{-3}	8.87×10^{-4}
1.05	1.57×10^{-2}	4.50×10^{-3}	4.49×10^{-4}
1.25	1.26×10^{-2}	2.98×10^{-3}	2.41×10^{-4}
1.45	9.87×10^{-3}	1.95×10^{-3}	1.36×10^{-4}
1.65	7.62×10^{-3}	1.27×10^{-3}	8.05×10^{-5}
1.85	5.73×10^{-3}	8.17×10^{-4}	4.87×10^{-5}
2.05	4.14×10^{-3}	5.13×10^{-4}	2.94×10^{-5}
2.25	2.80×10^{-3}	3.09×10^{-4}	1.74×10^{-5}
2.45	1.71×10^{-3}	1.71×10^{-4}	9.49×10^{-6}
2.65	8.43×10^{-4}	7.92×10^{-5}	4.33×10^{-6}
2.85	2.36×10^{-4}	2.12×10^{-5}	1.12×10^{-6}
$T_0 = 2.00 \text{ MeV}$			
0.05	2.79×10^{-2}	1.59×10^{-2}	5.40×10^{-3}
.15	2.15×10^{-2}	1.21×10^{-2}	3.98×10^{-3}
.25	1.81×10^{-2}	9.90×10^{-3}	3.12×10^{-3}
.35	1.56×10^{-2}	8.34×10^{-3}	2.42×10^{-3}
.45	1.35×10^{-2}	6.99×10^{-3}	1.85×10^{-3}
.65	1.02×10^{-2}	4.73×10^{-3}	9.46×10^{-4}
.85	7.42×10^{-3}	3.04×10^{-3}	4.44×10^{-4}
1.05	5.18×10^{-3}	1.83×10^{-3}	2.09×10^{-4}
1.25	3.37×10^{-3}	1.03×10^{-3}	9.70×10^{-5}
1.45	1.95×10^{-3}	5.21×10^{-4}	4.31×10^{-5}
1.65	9.01×10^{-4}	2.17×10^{-4}	1.67×10^{-5}
1.85	2.26×10^{-4}	5.11×10^{-5}	3.79×10^{-6}
Photon energy, MeV	Bremsstrahlung intensity, $\frac{\text{MeV}}{\text{MeV-sr-electron}}$		
	$\varphi_d = 0^\circ$	$\varphi_d = 30^\circ$	$\varphi_d = 60^\circ$
$T_0 = 1.00 \text{ MeV}$			
0.05	7.99×10^{-3}	6.27×10^{-3}	3.21×10^{-3}
.15	5.42×10^{-3}	4.20×10^{-3}	2.10×10^{-3}
.25	4.03×10^{-3}	3.07×10^{-3}	1.45×10^{-3}
.35	3.02×10^{-3}	2.25×10^{-3}	9.95×10^{-4}
.45	2.20×10^{-3}	1.59×10^{-3}	6.55×10^{-4}
.65	9.71×10^{-4}	6.45×10^{-4}	2.15×10^{-4}
.85	2.27×10^{-4}	1.38×10^{-4}	3.83×10^{-4}
$T_0 = 0.75 \text{ MeV}$			
0.05	4.40×10^{-3}	3.79×10^{-3}	2.39×10^{-3}
.15	2.75×10^{-3}	2.34×10^{-3}	1.44×10^{-3}
.25	1.86×10^{-3}	1.56×10^{-3}	9.09×10^{-4}
.35	1.23×10^{-3}	1.00×10^{-3}	5.52×10^{-4}
.45	7.36×10^{-4}	5.85×10^{-4}	3.06×10^{-4}
.65	1.15×10^{-4}	8.46×10^{-5}	3.79×10^{-5}
$T_0 = 0.50 \text{ MeV}$			
0.05	1.85×10^{-3}	1.73×10^{-3}	1.34×10^{-3}
.15	9.77×10^{-4}	9.00×10^{-4}	6.81×10^{-4}
.25	5.17×10^{-4}	4.67×10^{-4}	3.35×10^{-4}
.35	2.19×10^{-4}	1.93×10^{-4}	1.30×10^{-4}
.45	3.78×10^{-5}	3.25×10^{-5}	2.19×10^{-5}

TABLE VII.- THICK-TARGET BREMSSTRAHLUNG INTENSITY FOR TITANIUM

Photon energy, MeV	Bremsstrahlung intensity, MeV MeV-sr-electron		
	$\varphi_d = 0^\circ$	$\varphi_d = 30^\circ$	$\varphi_d = 60^\circ$
$T_0 = 3.00 \text{ MeV}$			
0.05	6.62×10^{-2}	4.40×10^{-2}	1.66×10^{-2}
.15	5.56×10^{-2}	3.58×10^{-2}	1.32×10^{-2}
.25	4.92×10^{-2}	3.09×10^{-2}	1.10×10^{-2}
.35	4.42×10^{-2}	2.72×10^{-2}	9.34×10^{-3}
.45	4.01×10^{-2}	2.42×10^{-2}	7.79×10^{-3}
.65	3.32×10^{-2}	1.87×10^{-2}	4.98×10^{-3}
.85	2.75×10^{-2}	1.41×10^{-2}	2.87×10^{-3}
1.05	2.25×10^{-2}	1.02×10^{-2}	1.57×10^{-3}
1.25	1.81×10^{-2}	7.17×10^{-3}	8.53×10^{-4}
1.45	1.44×10^{-2}	4.89×10^{-3}	4.72×10^{-4}
1.65	1.11×10^{-2}	3.26×10^{-3}	2.69×10^{-4}
1.85	8.37×10^{-3}	2.12×10^{-3}	1.56×10^{-4}
2.05	6.02×10^{-3}	1.33×10^{-3}	9.02×10^{-5}
2.25	4.40×10^{-3}	7.88×10^{-4}	5.07×10^{-5}
2.45	2.43×10^{-3}	4.25×10^{-4}	2.64×10^{-5}
2.65	1.18×10^{-3}	1.89×10^{-4}	1.14×10^{-5}
2.85	3.27×10^{-4}	4.74×10^{-5}	2.72×10^{-6}
$T_0 = 2.00 \text{ MeV}$			
0.05	3.80×10^{-2}	2.72×10^{-2}	1.10×10^{-2}
.15	2.98×10^{-2}	2.09×10^{-2}	8.23×10^{-3}
.25	2.53×10^{-2}	1.75×10^{-2}	6.66×10^{-3}
.35	2.18×10^{-2}	1.48×10^{-2}	5.36×10^{-3}
.45	1.90×10^{-2}	1.26×10^{-2}	4.29×10^{-3}
.65	1.44×10^{-2}	8.94×10^{-3}	2.51×10^{-3}
.85	1.07×10^{-2}	6.05×10^{-3}	1.34×10^{-3}
1.05	7.55×10^{-3}	3.84×10^{-3}	6.73×10^{-4}
1.25	4.97×10^{-3}	2.25×10^{-3}	3.19×10^{-4}
1.45	2.92×10^{-3}	1.18×10^{-3}	1.41×10^{-4}
1.65	1.38×10^{-3}	4.95×10^{-4}	5.28×10^{-5}
1.85	3.52×10^{-4}	1.15×10^{-4}	1.15×10^{-5}
Photon energy, MeV	Bremsstrahlung intensity, MeV MeV-sr-electron		
	$\varphi_d = 0^\circ$	$\varphi_d = 30^\circ$	$\varphi_d = 60^\circ$
$T_0 = 1.00 \text{ MeV}$			
0.05	1.05×10^{-2}	9.25×10^{-3}	5.80×10^{-3}
.15	7.11×10^{-3}	6.20×10^{-3}	3.83×10^{-3}
.25	5.28×10^{-3}	4.54×10^{-3}	2.72×10^{-3}
.35	3.96×10^{-3}	3.35×10^{-3}	1.92×10^{-3}
.45	2.90×10^{-3}	2.41×10^{-3}	1.30×10^{-3}
.65	1.31×10^{-3}	1.03×10^{-3}	4.77×10^{-4}
.85	3.17×10^{-4}	2.30×10^{-4}	9.22×10^{-5}
$T_0 = 0.75 \text{ MeV}$			
0.05	4.34×10^{-3}	4.05×10^{-3}	3.05×10^{-3}
.15	2.69×10^{-3}	2.48×10^{-3}	1.84×10^{-3}
.25	1.80×10^{-3}	1.65×10^{-3}	1.19×10^{-3}
.35	1.19×10^{-3}	1.07×10^{-3}	7.38×10^{-4}
.45	7.21×10^{-4}	6.33×10^{-4}	4.14×10^{-4}
.65	1.17×10^{-4}	9.66×10^{-5}	5.58×10^{-5}
$T_0 = 0.50 \text{ MeV}$			
0.05	1.25×10^{-3}	1.22×10^{-3}	1.09×10^{-3}
.15	6.41×10^{-4}	6.22×10^{-4}	5.50×10^{-3}
.25	3.33×10^{-4}	3.19×10^{-4}	2.75×10^{-4}
.35	1.40×10^{-4}	1.32×10^{-4}	1.09×10^{-4}
.45	2.44×10^{-5}	2.23×10^{-5}	1.77×10^{-5}

TABLE VIII.- THICK-TARGET BREMSSTRAHLUNG INTENSITY FOR MANGANESE

Photon energy, MeV	Bremsstrahlung intensity, $\frac{\text{MeV}}{\text{MeV-sr-electron}}$			Photon energy, MeV	Bremsstrahlung intensity, $\frac{\text{MeV}}{\text{MeV-sr-electron}}$				
	$\varphi_d = 0^\circ$	$\varphi_d = 30^\circ$	$\varphi_d = 60^\circ$		$\varphi_d = 0^\circ$	$\varphi_d = 30^\circ$	$\varphi_d = 60^\circ$		
$T_0 = 3.00 \text{ MeV}$						$T_0 = 1.00 \text{ MeV}$			
0.05	6.04×10^{-2}	4.47×10^{-2}	1.80×10^{-2}	0.05	1.04×10^{-2}	9.39×10^{-3}	6.13×10^{-3}		
.15	5.48×10^{-2}	3.85×10^{-2}	1.49×10^{-2}	.15	7.09×10^{-3}	6.33×10^{-3}	4.09×10^{-3}		
.25	5.01×10^{-2}	3.40×10^{-2}	1.27×10^{-2}	.25	5.26×10^{-3}	4.64×10^{-3}	2.93×10^{-3}		
.35	4.51×10^{-2}	3.00×10^{-2}	1.08×10^{-2}	.35	3.94×10^{-3}	3.42×10^{-3}	2.08×10^{-3}		
.45	4.10×10^{-2}	2.67×10^{-2}	9.11×10^{-3}	.45	2.89×10^{-3}	2.46×10^{-3}	1.42×10^{-3}		
.65	3.41×10^{-2}	2.09×10^{-2}	6.00×10^{-3}	.65	1.31×10^{-3}	1.06×10^{-3}	5.33×10^{-4}		
.85	2.83×10^{-2}	1.59×10^{-2}	3.59×10^{-3}	.85	3.18×10^{-4}	2.41×10^{-4}	1.05×10^{-4}		
1.05	2.32×10^{-2}	1.17×10^{-2}	2.01×10^{-3}	$T_0 = 0.75 \text{ MeV}$					
1.25	1.86×10^{-2}	8.23×10^{-3}	1.10×10^{-3}	0.05	4.33×10^{-3}	4.09×10^{-3}	3.18×10^{-3}		
1.45	1.47×10^{-2}	5.65×10^{-3}	6.03×10^{-4}	.15	2.68×10^{-3}	2.51×10^{-3}	1.93×10^{-3}		
1.65	1.14×10^{-2}	3.78×10^{-3}	3.41×10^{-4}	.25	1.79×10^{-3}	1.66×10^{-3}	1.25×10^{-3}		
1.85	8.57×10^{-3}	2.46×10^{-3}	1.96×10^{-4}	.35	1.18×10^{-3}	1.08×10^{-3}	7.79×10^{-4}		
2.05	6.16×10^{-3}	1.54×10^{-3}	1.12×10^{-4}	.45	7.14×10^{-4}	6.39×10^{-4}	4.40×10^{-4}		
2.25	4.14×10^{-3}	9.17×10^{-4}	6.29×10^{-5}	.65	1.16×10^{-4}	9.86×10^{-5}	6.06×10^{-5}		
2.45	2.49×10^{-3}	4.94×10^{-4}	3.26×10^{-5}	$T_0 = 0.50 \text{ MeV}$					
2.65	1.21×10^{-3}	2.18×10^{-4}	1.41×10^{-5}	0.05	1.26×10^{-3}	1.24×10^{-3}	1.12×10^{-3}		
2.85	3.33×10^{-4}	5.40×10^{-5}	3.31×10^{-6}	.15	6.45×10^{-4}	6.31×10^{-4}	5.70×10^{-4}		
$T_0 = 2.00 \text{ MeV}$						$T_0 = 1.00 \text{ MeV}$			
0.05	3.64×10^{-2}	2.77×10^{-2}	1.17×10^{-2}	.25	3.32×10^{-4}	3.21×10^{-4}	2.84×10^{-4}		
.15	2.99×10^{-2}	2.22×10^{-2}	9.17×10^{-3}	.35	1.39×10^{-4}	1.32×10^{-4}	1.13×10^{-4}		
.25	2.57×10^{-2}	1.88×10^{-2}	7.58×10^{-3}	.45	2.41×10^{-5}	2.24×10^{-5}	1.83×10^{-5}		
.35	2.23×10^{-2}	1.59×10^{-2}	6.14×10^{-3}						
.45	1.95×10^{-2}	1.36×10^{-2}	4.96×10^{-3}						
.65	1.48×10^{-2}	9.75×10^{-3}	2.99×10^{-3}						
.85	1.09×10^{-2}	6.67×10^{-3}	1.64×10^{-3}						
1.05	7.75×10^{-3}	4.27×10^{-3}	8.39×10^{-4}						
1.25	5.10×10^{-3}	2.52×10^{-3}	3.98×10^{-4}						
1.45	2.99×10^{-3}	1.32×10^{-3}	1.75×10^{-4}						
1.65	1.41×10^{-3}	5.53×10^{-4}	6.49×10^{-5}						
1.85	3.61×10^{-4}	1.28×10^{-4}	1.40×10^{-5}						

TABLE IX.- THICK-TARGET BREMSSTRAHLUNG INTENSITY FOR IRON

Photon energy, MeV	Bremsstrahlung intensity, MeV MeV-sr-electron		
	$\varphi_d = 0^\circ$	$\varphi_d = 30^\circ$	$\varphi_d = 60^\circ$
$T_0 = 3.00 \text{ MeV}$			
0.05	7.03×10^{-2}	5.14×10^{-2}	1.88×10^{-2}
.15	6.13×10^{-2}	4.29×10^{-2}	1.57×10^{-2}
.25	5.35×10^{-2}	3.69×10^{-2}	1.30×10^{-2}
.35	4.72×10^{-2}	3.22×10^{-2}	1.09×10^{-2}
.45	4.36×10^{-2}	2.88×10^{-2}	9.22×10^{-3}
.65	3.56×10^{-2}	2.23×10^{-2}	5.90×10^{-3}
.85	2.95×10^{-2}	1.70×10^{-2}	3.35×10^{-3}
1.05	2.43×10^{-2}	1.25×10^{-2}	1.91×10^{-3}
1.25	1.96×10^{-2}	8.93×10^{-3}	1.08×10^{-3}
1.45	1.56×10^{-2}	6.18×10^{-3}	6.26×10^{-4}
1.65	1.21×10^{-2}	4.17×10^{-3}	3.70×10^{-4}
1.85	9.10×10^{-3}	2.72×10^{-3}	2.22×10^{-4}
2.05	6.61×10^{-3}	1.73×10^{-3}	1.26×10^{-4}
2.25	4.61×10^{-3}	1.06×10^{-3}	6.73×10^{-5}
2.45	2.87×10^{-3}	5.92×10^{-4}	3.52×10^{-5}
2.65	1.44×10^{-3}	2.70×10^{-4}	1.51×10^{-5}
2.85	4.11×10^{-4}	6.88×10^{-5}	3.46×10^{-6}
$T_0 = 2.00 \text{ MeV}$			
0.05	4.01×10^{-2}	3.10×10^{-2}	1.25×10^{-2}
.15	3.20×10^{-2}	2.42×10^{-2}	9.78×10^{-3}
.25	2.65×10^{-2}	1.99×10^{-2}	7.87×10^{-3}
.35	2.31×10^{-2}	1.70×10^{-2}	6.34×10^{-3}
.45	1.99×10^{-2}	1.44×10^{-2}	5.10×10^{-3}
.65	1.52×10^{-2}	1.03×10^{-2}	3.03×10^{-3}
.85	1.13×10^{-2}	7.05×10^{-3}	1.61×10^{-3}
1.05	8.08×10^{-3}	4.55×10^{-3}	8.44×10^{-4}
1.25	5.35×10^{-3}	2.70×10^{-3}	4.15×10^{-4}
1.45	3.16×10^{-3}	1.43×10^{-3}	1.91×10^{-4}
1.65	1.49×10^{-3}	6.03×10^{-4}	7.59×10^{-5}
1.85	3.83×10^{-4}	1.40×10^{-4}	1.89×10^{-5}
Photon energy, MeV	Bremsstrahlung intensity, MeV MeV-sr-electron		
	$\varphi_d = 0^\circ$	$\varphi_d = 30^\circ$	$\varphi_d = 60^\circ$
$T_0 = 1.00 \text{ MeV}$			
0.05	1.04×10^{-2}	9.82×10^{-3}	6.57×10^{-3}
.15	7.06×10^{-3}	6.58×10^{-3}	4.37×10^{-3}
.25	5.18×10^{-3}	4.78×10^{-3}	3.10×10^{-3}
.35	3.84×10^{-3}	3.50×10^{-3}	2.19×10^{-3}
.45	2.79×10^{-3}	2.51×10^{-3}	1.49×10^{-3}
.65	1.33×10^{-3}	1.10×10^{-4}	5.52×10^{-4}
.85	3.31×10^{-4}	2.50×10^{-4}	1.05×10^{-4}
$T_0 = 0.75 \text{ MeV}$			
0.05	5.29×10^{-3}	5.35×10^{-3}	4.37×10^{-3}
.15	3.26×10^{-3}	3.27×10^{-3}	2.66×10^{-3}
.25	2.14×10^{-3}	2.14×10^{-3}	1.71×10^{-3}
.35	1.38×10^{-3}	1.37×10^{-3}	1.06×10^{-3}
.45	8.06×10^{-4}	7.98×10^{-4}	5.97×10^{-4}
.65	1.44×10^{-4}	1.27×10^{-4}	8.26×10^{-5}
$T_0 = 0.50 \text{ MeV}$			
0.05	2.41×10^{-3}	2.40×10^{-3}	2.22×10^{-3}
.15	1.25×10^{-3}	1.23×10^{-3}	1.13×10^{-3}
.25	6.42×10^{-4}	6.26×10^{-4}	5.62×10^{-4}
.35	2.66×10^{-4}	2.54×10^{-4}	2.21×10^{-4}
.45	4.58×10^{-5}	4.28×10^{-5}	3.58×10^{-5}

TABLE X.- THICK-TARGET BREMSSTRAHLUNG INTENSITY FOR NICKEL

Photon energy, MeV	Bremsstrahlung intensity, $\frac{\text{MeV}}{\text{MeV}\cdot\text{sr}\cdot\text{electron}}$			Photon energy, MeV	Bremsstrahlung intensity, $\frac{\text{MeV}}{\text{MeV}\cdot\text{sr}\cdot\text{electron}}$				
	$\varphi_d = 0^\circ$	$\varphi_d = 30^\circ$	$\varphi_d = 60^\circ$		$\varphi_d = 0^\circ$	$\varphi_d = 30^\circ$	$\varphi_d = 60^\circ$		
$T_0 = 3.00 \text{ MeV}$									
0.05	7.09×10^{-2}	5.41×10^{-2}	2.15×10^{-2}	0.05	1.13×10^{-2}	1.03×10^{-2}	6.97×10^{-3}		
.15	6.34×10^{-2}	4.63×10^{-2}	1.81×10^{-2}	.15	7.73×10^{-3}	7.02×10^{-3}	4.73×10^{-3}		
.25	5.76×10^{-2}	4.11×10^{-2}	1.56×10^{-2}	.25	5.75×10^{-3}	5.17×10^{-3}	3.41×10^{-3}		
.35	5.19×10^{-2}	3.63×10^{-2}	1.33×10^{-2}	.35	4.30×10^{-3}	3.81×10^{-3}	2.43×10^{-3}		
.45	4.72×10^{-2}	3.24×10^{-2}	1.13×10^{-2}	.45	3.15×10^{-3}	2.75×10^{-3}	1.67×10^{-3}		
.65	3.92×10^{-2}	2.55×10^{-2}	7.63×10^{-3}	.65	1.43×10^{-3}	1.19×10^{-3}	6.39×10^{-4}		
.85	3.26×10^{-2}	1.97×10^{-2}	4.75×10^{-3}	.85	3.51×10^{-4}	2.72×10^{-4}	1.29×10^{-4}		
1.05	2.69×10^{-2}	1.47×10^{-2}	2.77×10^{-3}	$T_0 = 1.00 \text{ MeV}$					
1.25	2.18×10^{-2}	1.06×10^{-2}	1.57×10^{-3}	0.05	4.71×10^{-3}	4.51×10^{-3}	3.59×10^{-3}		
1.45	1.73×10^{-2}	7.42×10^{-3}	8.84×10^{-4}	.15	2.92×10^{-3}	2.78×10^{-3}	2.20×10^{-3}		
1.65	1.34×10^{-2}	4.99×10^{-3}	4.96×10^{-4}	.25	1.96×10^{-3}	1.84×10^{-3}	1.43×10^{-3}		
1.85	1.01×10^{-2}	3.26×10^{-3}	2.82×10^{-4}	.35	1.28×10^{-3}	1.19×10^{-3}	8.94×10^{-4}		
2.05	7.25×10^{-3}	2.05×10^{-3}	1.60×10^{-4}	.45	7.75×10^{-4}	7.05×10^{-4}	5.08×10^{-4}		
2.25	4.88×10^{-3}	1.22×10^{-3}	8.86×10^{-5}	.65	1.27×10^{-4}	1.10×10^{-4}	7.10×10^{-5}		
2.45	2.93×10^{-3}	6.57×10^{-4}	4.53×10^{-5}	$T_0 = 0.75 \text{ MeV}$					
2.65	1.43×10^{-3}	2.89×10^{-4}	1.91×10^{-5}	0.05	1.39×10^{-3}	1.38×10^{-3}	1.27×10^{-3}		
2.85	3.94×10^{-4}	7.11×10^{-5}	4.46×10^{-6}	.15	7.12×10^{-4}	7.01×10^{-4}	6.44×10^{-4}		
$T_0 = 2.00 \text{ MeV}$									
0.05	4.19×10^{-2}	3.28×10^{-2}	1.40×10^{-2}	.25	3.65×10^{-4}	3.55×10^{-4}	3.21×10^{-4}		
.15	3.42×10^{-2}	2.62×10^{-2}	1.11×10^{-2}	.35	1.51×10^{-4}	1.45×10^{-4}	1.27×10^{-4}		
.25	2.94×10^{-2}	2.23×10^{-2}	9.26×10^{-3}	.45	2.62×10^{-5}	2.45×10^{-5}	2.07×10^{-5}		
.35	2.54×10^{-2}	1.89×10^{-2}	7.54×10^{-3}						
.45	2.22×10^{-2}	1.62×10^{-2}	6.15×10^{-3}						
.65	1.69×10^{-2}	1.17×10^{-2}	3.81×10^{-3}						
.85	1.26×10^{-2}	8.11×10^{-3}	2.17×10^{-3}						
1.05	9.02×10^{-3}	5.31×10^{-3}	1.15×10^{-3}						
1.25	6.01×10^{-3}	3.20×10^{-3}	5.66×10^{-4}						
1.45	3.56×10^{-3}	1.70×10^{-3}	2.53×10^{-4}						
1.65	1.67×10^{-3}	7.14×10^{-4}	9.33×10^{-5}						
1.85	4.25×10^{-4}	1.63×10^{-4}	1.97×10^{-5}						

TABLE XI.- THICK-TARGET BREMSSTRAHLUNG INTENSITY FOR COPPER

Photon energy, MeV	Bremsstrahlung intensity, $\frac{\text{MeV}}{\text{MeV-sr-electron}}$		
	$\varphi_d = 0^\circ$	$\varphi_d = 30^\circ$	$\varphi_d = 60^\circ$
$T_0 = 3.00 \text{ MeV}$			
0.05	6.50×10^{-2}	5.10×10^{-2}	2.09×10^{-2}
.15	5.98×10^{-2}	4.48×10^{-2}	1.80×10^{-2}
.25	5.50×10^{-2}	4.01×10^{-2}	1.57×10^{-2}
.35	4.95×10^{-2}	3.54×10^{-2}	1.33×10^{-2}
.45	4.50×10^{-2}	3.16×10^{-2}	1.13×10^{-2}
.65	3.75×10^{-2}	2.49×10^{-2}	7.71×10^{-3}
.85	3.11×10^{-2}	1.92×10^{-2}	4.81×10^{-3}
1.05	2.56×10^{-2}	1.44×10^{-2}	2.81×10^{-3}
1.25	2.08×10^{-2}	1.04×10^{-2}	1.59×10^{-3}
1.45	1.65×10^{-2}	7.27×10^{-3}	8.94×10^{-4}
1.65	1.29×10^{-2}	4.95×10^{-3}	5.08×10^{-4}
1.85	9.70×10^{-3}	3.26×10^{-3}	2.92×10^{-4}
2.05	6.98×10^{-3}	2.05×10^{-3}	1.66×10^{-4}
2.25	4.69×10^{-3}	1.22×10^{-3}	9.18×10^{-5}
2.45	2.82×10^{-3}	6.55×10^{-4}	4.69×10^{-5}
2.65	1.37×10^{-3}	2.87×10^{-4}	2.00×10^{-5}
2.85	3.77×10^{-4}	7.02×10^{-5}	4.85×10^{-6}
$T_0 = 2.00 \text{ MeV}$			
0.05	3.91×10^{-2}	3.12×10^{-2}	1.36×10^{-2}
.15	3.24×10^{-2}	2.54×10^{-2}	1.10×10^{-2}
.25	2.81×10^{-2}	2.17×10^{-2}	9.28×10^{-3}
.35	2.43×10^{-2}	1.84×10^{-2}	7.55×10^{-3}
.45	2.12×10^{-2}	1.58×10^{-2}	6.17×10^{-3}
.65	1.61×10^{-2}	1.14×10^{-2}	3.83×10^{-3}
.85	1.20×10^{-2}	7.87×10^{-3}	2.18×10^{-3}
1.05	8.52×10^{-3}	5.12×10^{-3}	1.15×10^{-3}
1.25	5.66×10^{-3}	3.08×10^{-3}	5.63×10^{-4}
1.45	3.36×10^{-3}	1.64×10^{-3}	2.52×10^{-4}
1.65	1.59×10^{-3}	6.97×10^{-4}	9.42×10^{-5}
1.85	4.11×10^{-4}	1.61×10^{-4}	2.01×10^{-5}
Photon energy, MeV	Bremsstrahlung intensity, $\frac{\text{MeV}}{\text{MeV-sr-electron}}$		
	$\varphi_d = 0^\circ$	$\varphi_d = 30^\circ$	$\varphi_d = 60^\circ$
$T_0 = 1.00 \text{ MeV}$			
0.05	1.10×10^{-2}	1.01×10^{-2}	6.82×10^{-3}
.15	7.53×10^{-3}	6.89×10^{-3}	4.69×10^{-3}
.25	5.61×10^{-3}	5.08×10^{-3}	3.40×10^{-3}
.35	4.19×10^{-3}	3.74×10^{-3}	2.42×10^{-3}
.45	3.07×10^{-3}	2.70×10^{-3}	1.67×10^{-3}
.65	1.40×10^{-3}	1.17×10^{-3}	6.43×10^{-4}
.85	3.41×10^{-4}	2.68×10^{-4}	1.29×10^{-4}
$T_0 = 0.75 \text{ MeV}$			
0.05	4.60×10^{-3}	4.42×10^{-3}	3.52×10^{-3}
.15	2.86×10^{-3}	2.73×10^{-3}	2.18×10^{-3}
.25	1.91×10^{-3}	1.81×10^{-3}	1.42×10^{-3}
.35	1.25×10^{-3}	1.17×10^{-3}	8.87×10^{-4}
.45	7.57×10^{-4}	6.92×10^{-4}	5.05×10^{-4}
.65	1.24×10^{-4}	1.08×10^{-4}	7.10×10^{-5}
$T_0 = 0.50 \text{ MeV}$			
0.05	1.37×10^{-3}	1.36×10^{-3}	1.26×10^{-3}
.15	7.01×10^{-4}	6.92×10^{-4}	6.38×10^{-4}
.25	3.58×10^{-4}	3.50×10^{-4}	3.18×10^{-4}
.35	1.48×10^{-4}	1.42×10^{-4}	1.25×10^{-4}
.45	2.55×10^{-5}	2.40×10^{-5}	2.04×10^{-5}

TABLE XII.- THICK-TARGET BREMSSTRAHLUNG INTENSITY FOR TUNGSTEN

Photon energy, MeV	Bremsstrahlung intensity, $\frac{\text{MeV}}{\text{MeV}\cdot\text{sr}\cdot\text{electron}}$		
	$\varphi_d = 0^\circ$	$\varphi_d = 30^\circ$	$\varphi_d = 60^\circ$
$T_0 = 3.00 \text{ MeV}$			
0.05	6.96×10^{-3}	7.20×10^{-3}	5.94×10^{-3}
.15	1.77×10^{-2}	1.48×10^{-2}	8.46×10^{-3}
.25	7.38×10^{-2}	4.98×10^{-2}	2.41×10^{-2}
.35	8.54×10^{-2}	5.61×10^{-2}	2.70×10^{-2}
.45	8.91×10^{-2}	5.76×10^{-2}	2.77×10^{-2}
.65	7.79×10^{-2}	4.89×10^{-2}	2.21×10^{-2}
.85	6.63×10^{-2}	4.02×10^{-2}	1.66×10^{-2}
1.05	5.56×10^{-2}	3.23×10^{-2}	1.19×10^{-2}
1.25	4.61×10^{-2}	2.54×10^{-2}	8.11×10^{-3}
1.45	3.75×10^{-2}	1.94×10^{-2}	5.33×10^{-3}
1.65	2.97×10^{-2}	1.43×10^{-2}	3.36×10^{-3}
1.85	2.28×10^{-2}	1.02×10^{-2}	2.05×10^{-3}
2.05	1.67×10^{-2}	6.85×10^{-3}	1.20×10^{-3}
2.25	1.14×10^{-2}	4.29×10^{-3}	6.61×10^{-4}
2.45	6.88×10^{-3}	2.38×10^{-3}	3.30×10^{-4}
2.65	3.30×10^{-3}	1.06×10^{-3}	1.34×10^{-4}
2.85	8.47×10^{-4}	2.54×10^{-4}	2.93×10^{-5}
$T_0 = 2.00 \text{ MeV}$			
0.05	5.61×10^{-3}	5.06×10^{-3}	3.53×10^{-3}
.15	1.24×10^{-2}	9.81×10^{-3}	5.02×10^{-3}
.25	3.24×10^{-2}	2.56×10^{-2}	1.40×10^{-2}
.35	3.28×10^{-2}	2.59×10^{-2}	1.47×10^{-2}
.45	3.11×10^{-2}	2.45×10^{-2}	1.42×10^{-2}
.65	2.42×10^{-2}	1.87×10^{-2}	1.03×10^{-2}
.85	1.82×10^{-2}	1.37×10^{-2}	6.91×10^{-3}
1.05	1.31×10^{-2}	9.49×10^{-3}	4.30×10^{-3}
1.25	8.77×10^{-3}	6.10×10^{-3}	2.45×10^{-3}
1.45	5.25×10^{-3}	3.47×10^{-3}	1.23×10^{-3}
1.65	2.50×10^{-3}	1.56×10^{-3}	4.86×10^{-4}
1.85	6.33×10^{-4}	3.74×10^{-4}	1.03×10^{-4}

Photon energy, MeV	Bremsstrahlung intensity, $\frac{\text{MeV}}{\text{MeV}\cdot\text{sr}\cdot\text{electron}}$		
	$\varphi_d = 0^\circ$	$\varphi_d = 30^\circ$	$\varphi_d = 60^\circ$
$T_0 = 1.00 \text{ MeV}$			
0.05	3.99×10^{-3}	3.47×10^{-3}	2.06×10^{-3}
.15	5.31×10^{-3}	4.70×10^{-3}	2.73×10^{-3}
.25	6.49×10^{-3}	6.10×10^{-3}	4.73×10^{-3}
.35	5.04×10^{-3}	4.76×10^{-3}	3.84×10^{-3}
.45	3.74×10^{-3}	3.53×10^{-3}	2.89×10^{-3}
.65	1.67×10^{-3}	1.55×10^{-3}	1.22×10^{-3}
.85	4.13×10^{-4}	3.74×10^{-4}	2.73×10^{-4}
$T_0 = 0.75 \text{ MeV}$			
0.05	2.60×10^{-3}	2.31×10^{-3}	1.39×10^{-3}
.15	2.61×10^{-3}	2.41×10^{-3}	1.59×10^{-3}
.25	2.41×10^{-3}	2.33×10^{-3}	2.00×10^{-3}
.35	1.57×10^{-3}	1.53×10^{-3}	1.35×10^{-3}
.45	9.30×10^{-4}	9.03×10^{-4}	8.06×10^{-4}
.65	1.46×10^{-4}	1.40×10^{-4}	1.19×10^{-4}
$T_0 = 0.50 \text{ MeV}$			
0.05	1.34×10^{-3}	1.23×10^{-3}	8.13×10^{-4}
.15	9.07×10^{-4}	8.66×10^{-4}	6.65×10^{-4}
.25	5.46×10^{-4}	5.38×10^{-4}	4.98×10^{-4}
.35	2.15×10^{-4}	2.13×10^{-4}	2.01×10^{-4}
.45	3.48×10^{-5}	3.43×10^{-5}	3.28×10^{-5}

TABLE XIII.- THICK-TARGET BREMSSTRAHLUNG INTENSITY FOR GOLD

Photon energy, MeV	Bremsstrahlung intensity, $\frac{\text{MeV}}{\text{MeV-sr-electron}}$		
	$\varphi_d = 0^\circ$	$\varphi_d = 30^\circ$	$\varphi_d = 60^\circ$
$T_0 = 3.00 \text{ MeV}$			
0.05	6.07×10^{-3}	6.51×10^{-3}	6.19×10^{-3}
.15	1.38×10^{-2}	1.21×10^{-2}	7.31×10^{-3}
.25	6.45×10^{-2}	4.50×10^{-2}	2.21×10^{-2}
.35	8.08×10^{-2}	5.45×10^{-2}	2.66×10^{-2}
.45	8.85×10^{-2}	5.85×10^{-2}	2.87×10^{-2}
.65	7.83×10^{-2}	5.03×10^{-2}	2.33×10^{-2}
.85	6.65×10^{-2}	4.14×10^{-2}	1.76×10^{-2}
1.05	5.63×10^{-2}	3.36×10^{-2}	1.28×10^{-2}
1.25	4.66×10^{-2}	2.64×10^{-2}	8.82×10^{-3}
1.45	3.79×10^{-2}	2.03×10^{-2}	5.83×10^{-3}
1.65	3.01×10^{-2}	1.50×10^{-2}	3.71×10^{-3}
1.85	2.32×10^{-2}	1.07×10^{-2}	2.27×10^{-3}
2.05	1.70×10^{-2}	7.22×10^{-3}	1.34×10^{-3}
2.25	1.17×10^{-2}	4.53×10^{-3}	7.40×10^{-4}
2.45	6.99×10^{-3}	2.52×10^{-3}	3.70×10^{-4}
2.65	3.36×10^{-3}	1.12×10^{-3}	1.50×10^{-4}
2.85	8.60×10^{-4}	2.68×10^{-4}	3.26×10^{-5}
$T_0 = 2.00 \text{ MeV}$			
0.05	5.08×10^{-3}	4.71×10^{-3}	3.65×10^{-3}
.15	1.05×10^{-2}	8.46×10^{-3}	4.48×10^{-3}
.25	3.11×10^{-2}	2.47×10^{-2}	1.34×10^{-2}
.35	3.31×10^{-2}	2.64×10^{-2}	1.50×10^{-2}
.45	3.24×10^{-2}	2.59×10^{-2}	1.52×10^{-2}
.65	2.53×10^{-2}	1.99×10^{-2}	1.11×10^{-2}
.85	1.90×10^{-2}	1.45×10^{-2}	7.54×10^{-3}
1.05	1.37×10^{-2}	1.02×10^{-2}	4.78×10^{-3}
1.25	9.24×10^{-3}	6.55×10^{-3}	2.74×10^{-3}
1.45	5.53×10^{-3}	3.74×10^{-3}	1.38×10^{-3}
1.65	2.63×10^{-3}	1.69×10^{-3}	5.50×10^{-4}
1.85	6.70×10^{-4}	4.06×10^{-4}	1.17×10^{-4}

Photon energy, MeV	Bremsstrahlung intensity, $\frac{\text{MeV}}{\text{MeV-sr-electron}}$		
	$\varphi_d = 0^\circ$	$\varphi_d = 30^\circ$	$\varphi_d = 60^\circ$
$T_0 = 1.00 \text{ MeV}$			
0.05	3.55×10^{-3}	3.13×10^{-3}	2.01×10^{-3}
.15	4.79×10^{-3}	4.22×10^{-3}	2.42×10^{-3}
.25	6.37×10^{-3}	5.97×10^{-3}	4.54×10^{-3}
.35	5.04×10^{-3}	4.77×10^{-3}	3.84×10^{-3}
.45	3.79×10^{-3}	3.59×10^{-3}	2.97×10^{-3}
.65	1.69×10^{-3}	1.58×10^{-3}	1.25×10^{-3}
.85	4.17×10^{-4}	3.80×10^{-4}	2.83×10^{-4}
$T_0 = 0.75 \text{ MeV}$			
0.05	2.39×10^{-3}	2.13×10^{-3}	1.35×10^{-3}
.15	2.49×10^{-3}	2.28×10^{-3}	1.47×10^{-3}
.25	2.43×10^{-3}	2.35×10^{-3}	1.98×10^{-3}
.35	1.60×10^{-3}	1.55×10^{-3}	1.37×10^{-3}
.45	9.51×10^{-4}	9.25×10^{-4}	8.29×10^{-4}
.65	1.48×10^{-4}	1.42×10^{-4}	1.23×10^{-4}
$T_0 = 0.50 \text{ MeV}$			
0.05	1.29×10^{-3}	1.19×10^{-3}	7.96×10^{-4}
.15	9.18×10^{-4}	8.72×10^{-4}	6.55×10^{-4}
.25	5.70×10^{-4}	5.62×10^{-4}	5.15×10^{-4}
.35	2.25×10^{-4}	2.22×10^{-4}	2.10×10^{-4}
.45	3.63×10^{-5}	3.59×10^{-5}	3.43×10^{-5}

TABLE XIV.- THICK-TARGET BREMSSTRAHLUNG INTENSITY FOR LEAD

Photon energy, MeV	Bremsstrahlung intensity, $\frac{\text{MeV}}{\text{MeV}\cdot\text{sr}\cdot\text{electron}}$			Photon energy, MeV	Bremsstrahlung intensity, $\frac{\text{MeV}}{\text{MeV}\cdot\text{sr}\cdot\text{electron}}$		
	$\varphi_d = 0^\circ$	$\varphi_d = 30^\circ$	$\varphi_d = 60^\circ$		$\varphi_d = 0^\circ$	$\varphi_d = 30^\circ$	$\varphi_d = 60^\circ$
$T_0 = 3.00 \text{ MeV}$							
0.05	5.17×10^{-3}	5.63×10^{-3}	5.35×10^{-3}	0.05	2.82×10^{-3}	2.48×10^{-3}	1.56×10^{-3}
.15	1.01×10^{-2}	9.32×10^{-3}	5.95×10^{-3}	.15	3.90×10^{-3}	3.39×10^{-3}	1.82×10^{-3}
.25	5.53×10^{-2}	3.93×10^{-2}	1.93×10^{-2}	.25	5.97×10^{-3}	5.57×10^{-3}	4.09×10^{-3}
.35	7.31×10^{-2}	5.00×10^{-2}	2.43×10^{-2}	.35	4.85×10^{-3}	4.57×10^{-3}	3.59×10^{-3}
.45	8.35×10^{-2}	5.59×10^{-2}	2.74×10^{-2}	.45	3.70×10^{-3}	3.50×10^{-3}	2.86×10^{-3}
.65	7.61×10^{-2}	4.95×10^{-2}	2.31×10^{-2}	.65	1.66×10^{-3}	1.56×10^{-3}	1.23×10^{-3}
.85	6.61×10^{-2}	4.16×10^{-2}	1.80×10^{-2}	.85	4.12×10^{-4}	3.77×10^{-4}	2.81×10^{-4}
1.05	5.58×10^{-2}	3.38×10^{-2}	1.31×10^{-2}	$T_0 = 1.00 \text{ MeV}$			
1.25	4.62×10^{-2}	2.66×10^{-2}	9.05×10^{-3}	0.05	1.91×10^{-3}	1.69×10^{-3}	1.03×10^{-3}
1.45	3.77×10^{-2}	2.04×10^{-2}	6.02×10^{-3}	.15	2.10×10^{-3}	1.89×10^{-3}	1.11×10^{-3}
1.65	2.99×10^{-2}	1.52×10^{-2}	3.85×10^{-3}	.25	2.32×10^{-3}	2.23×10^{-3}	1.81×10^{-3}
1.85	2.31×10^{-2}	1.08×10^{-2}	2.37×10^{-3}	.35	1.56×10^{-3}	1.51×10^{-3}	1.30×10^{-3}
2.05	1.69×10^{-2}	7.32×10^{-3}	1.40×10^{-3}	.45	9.37×10^{-4}	9.11×10^{-4}	8.08×10^{-4}
2.25	1.15×10^{-2}	4.60×10^{-3}	7.74×10^{-4}	.65	1.47×10^{-4}	1.41×10^{-4}	1.21×10^{-4}
2.45	6.95×10^{-3}	2.56×10^{-3}	3.87×10^{-4}	$T_0 = 0.75 \text{ MeV}$			
2.65	3.34×10^{-3}	1.14×10^{-3}	1.57×10^{-4}	0.05	1.07×10^{-3}	9.65×10^{-4}	6.01×10^{-4}
2.85	8.58×10^{-4}	2.73×10^{-4}	3.41×10^{-5}	.15	8.04×10^{-4}	7.50×10^{-4}	5.11×10^{-4}
$T_0 = 2.00 \text{ MeV}$							
0.05	4.21×10^{-3}	3.96×10^{-3}	3.06×10^{-3}	.25	5.50×10^{-4}	5.39×10^{-4}	4.78×10^{-4}
.15	7.87×10^{-3}	6.51×10^{-3}	3.55×10^{-3}	.35	2.21×10^{-4}	2.18×10^{-4}	2.01×10^{-4}
.25	2.78×10^{-2}	2.21×10^{-2}	1.18×10^{-2}	.45	3.61×10^{-5}	3.56×10^{-5}	3.36×10^{-5}
.35	3.10×10^{-2}	2.48×10^{-2}	1.39×10^{-2}				
.45	3.13×10^{-2}	2.51×10^{-2}	1.47×10^{-2}				
.65	2.50×10^{-2}	1.98×10^{-2}	1.11×10^{-2}				
.85	1.91×10^{-2}	1.47×10^{-2}	7.74×10^{-3}				
1.05	1.38×10^{-2}	1.03×10^{-2}	4.91×10^{-3}				
1.25	9.25×10^{-3}	6.62×10^{-3}	2.82×10^{-3}				
1.45	5.55×10^{-3}	3.79×10^{-3}	1.43×10^{-3}				
1.65	2.64×10^{-3}	1.71×10^{-3}	5.72×10^{-4}				
1.85	6.72×10^{-4}	4.12×10^{-4}	1.22×10^{-4}				

NATIONAL AERONAUTICS AND SPACE ADMINISTRATION
WASHINGTON, D.C. 20546
OFFICIAL BUSINESS

POSTAGE AND FEES PAID
NATIONAL AERONAUTICS AND
SPACE ADMINISTRATION

FIRST CLASS MAIL

POSTMASTER: If Undeliverable (Section 158
Postal Manual) Do Not Return

"The aeronautical and space activities of the United States shall be conducted so as to contribute . . . to the expansion of human knowledge of phenomena in the atmosphere and space. The Administration shall provide for the widest practicable and appropriate dissemination of information concerning its activities and the results thereof."

— NATIONAL AERONAUTICS AND SPACE ACT OF 1958

NASA SCIENTIFIC AND TECHNICAL PUBLICATIONS

TECHNICAL REPORTS: Scientific and technical information considered important, complete, and a lasting contribution to existing knowledge.

TECHNICAL NOTES: Information less broad in scope but nevertheless of importance as a contribution to existing knowledge.

TECHNICAL MEMORANDUMS: Information receiving limited distribution because of preliminary data, security classification, or other reasons.

CONTRACTOR REPORTS: Scientific and technical information generated under a NASA contract or grant and considered an important contribution to existing knowledge.

TECHNICAL TRANSLATIONS: Information published in a foreign language considered to merit NASA distribution in English.

SPECIAL PUBLICATIONS: Information derived from or of value to NASA activities. Publications include conference proceedings, monographs, data compilations, handbooks, sourcebooks, and special bibliographies.

TECHNOLOGY UTILIZATION PUBLICATIONS: Information on technology used by NASA that may be of particular interest in commercial and other non-aerospace applications. Publications include Tech Briefs, Technology Utilization Reports and Notes, and Technology Surveys.

Details on the availability of these publications may be obtained from:

SCIENTIFIC AND TECHNICAL INFORMATION DIVISION
NATIONAL AERONAUTICS AND SPACE ADMINISTRATION
Washington, D.C. 20546